

Aromatic Nanosandwich Obtained by σ -Dimerization of a Nanographenoid π -Radical

Supplementary Information

by Liliia Moshniah, Marika Żyła-Karwowska,
Piotr J. Chmielewski, Tadeusz Lis, Joanna Cybińska, Elżbieta Gońska,
Johannes Oschwald, Thomas Drewello, Samara Medina Rivero, Juan Casado,
and Marcin Stępień*

Table of Contents

Experimental	2
Synthesis.....	4
Additional Figures.....	10
Additional Tables.....	29
NMR Spectra.....	39
Mass Spectra	43
References.....	45

Experimental

General. Tetrahydrofuran, toluene and N,N-dimethylformamide were dried using a commercial solvent purification system. Dichloromethane and chloroform were distilled from calcium hydride when used as reaction solvents. Deuterated camphorsulfonic acid-*d* was obtained by recrystallization of camphorsulfonic acid from deuterated water and acetic acid-*d*. All other solvents and reagents were used as received. Compound **5** was synthesized as previously reported.¹

¹H NMR spectra were recorded on high-field spectrometers (¹H frequency 500.13 or 600.13 MHz), equipped with broadband inverse or conventional gradient probe heads. Spectra were referenced to the residual solvent signals (chloroform-*d* 7.24 ppm; toluene-*d*₈ 2.09 ppm). Two-dimensional NMR spectra were recorded with 2048 data points in the *t*₂ domain and up to 2048 points in the *t*₁ domain, with a 1.5 s recovery delay. All 2D spectra were recorded with gradient selection, with the exception of NOESY and ROESY. NOESY mixing time and ROESY spinlock time were 500 ms and 300 ms, respectively. ¹³C NMR spectra were recorded with ¹H broadband decoupling and referenced to solvent signals (¹³CDCl₃, 77.0 ppm).

High-resolution mass spectra were recorded using MALDI ionization in the positive mode. MALDI-ToF-MS was performed with a Bruker ultraflexXtreme in the positive-ion mode, using trans-2-[3-(4-*tert*-butylphenyl)-2-methyl-2-propenylidene]malonitrile (DCTB) as the matrix. The matrix-to-analyte ratio was 40:1.

Electrochemical measurements (dichloromethane, 293 K) were performed on an EA9C Multifunctional Electrochemical Analyzer using a glassy-carbon working electrode, platinum wire as the auxiliary electrode, and silver wire as a reference electrode. The voltammograms were referenced against the half-wave potential of Fc⁺/Fc.

Photoluminescence excitation (PLE) and emission (PL) spectra as well as decay kinetics (DEC) were taken with the FSL980-sm Fluorescence Spectrometer from Edinburgh Instruments Ltd. A 450 W Xenon arc lamp (PL and PLE) and a Super Continuum Fianium laser were used as excitation sources. Emission spectra were corrected for the recording system efficiency and excitation spectra were corrected for the incident light intensity. PLE and PL spectra and QY were measured using cooled extended red Hamamatsu photomultiplier operating in range 200 – 1050 nm. Quantum yield measurements were performed by using an Edinburgh Instruments integrating sphere equipped with a small elliptical mirror and a baffle plate for beam steering and shielding against directly detected light. For the measurement, the integrating sphere replaces the standard sample holder inside the sample chamber. Calculations of quantum yields were made using the software provided by Edinburgh Instruments.

Irradiation of compound **4₂.** Absorption spectroscopy: Absorption spectra were recorded using a Varian Cary 60 spectrophotometer. A toluene solution of **4**₂ was degassed with freeze-pump-thaw cycles and introduced into a glovebox. In the glovebox, the solution was transferred to a 1 mm quartz cuvette and kept in darkness. After that the cuvette was transferred to the measurement chamber of the spectrophotometer. After the first spectrum was recorded, the sample was irradiated with a UV lamp (365 nm) for 10 seconds, and the second spectrum was recorded immediately. 8 steps of irradiation were performed (the total time of irradiation was 80 seconds). The solution was irradiated until no further change of the electronic spectrum was observed. Once the experiment was finished, the sample was protected from light and introduced to the glovebox. After 12 h in darkness the experiment was repeated using the same condition on the same sample two more times. After that,

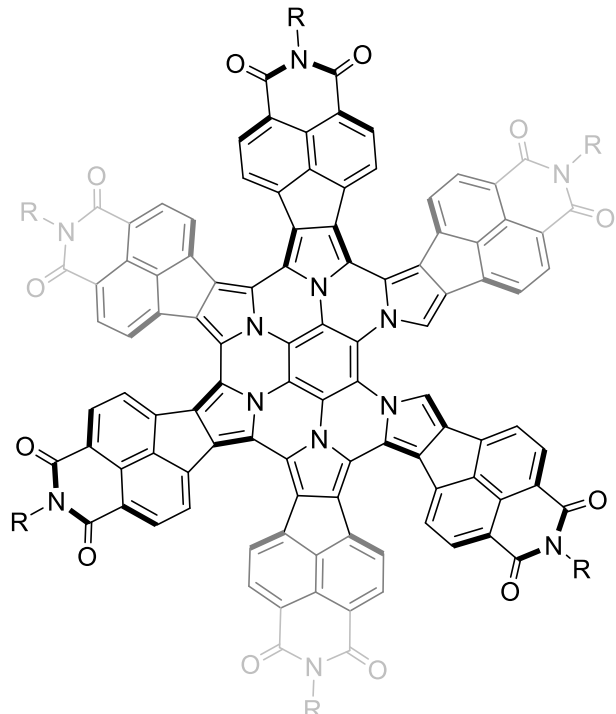
the same sample was irradiated with a LED lamp, observing the same changes in the spectra. (ESR spectra) A degassed solution of **4₂** in toluene was transferred under inert conditions to a quartz test tube and protected from atmosphere and light. After the first ESR measurement was made, the solution was irradiated with a UV lamp for 5 minutes and a new ESR spectrum was recorded immediately; the irradiation of the sample was repeated 2 times using a UV lamp (365 nm) and then 2 times using a consumer white-light LED lamp. After all irradiation cycles were performed, kinetics of the radical decay were monitored over the course of 90 minutes.

Computational methods. Density functional theory (DFT) calculations were performed using Gaussian 16.² DFT geometry optimizations were carried out in unconstrained *C₁* symmetry, using molecular mechanics or semi-empirical models as starting geometries. DFT geometries were refined to meet standard convergence criteria, and the existence of a local minimum was verified by a normal mode frequency calculation. Geometry optimizations, frequency calculations were performed using the hybrid functionals B3LYP and ωB97XD and the 6-31G(d,p) basis set (3-21G for **4₂**).^{3–6} For compound **7** 50 electronic transitions, and for **4₂** and **4^{*}** 200 electronic transitions were calculated by means of time-dependent DFT (TD-DFT)⁷, using the hybrid functional B3LYP and the 6-31G(d,p) basis set (3-21G for **4₂**). The same approach was also used for calculation of HOMO and LUMO energies.

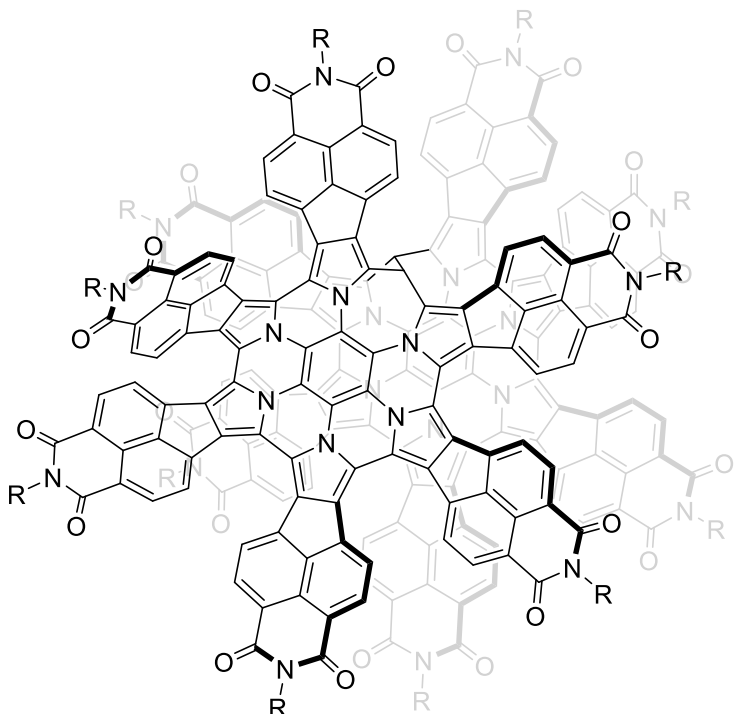
Tight-binding density functional theory calculations were performed using xTB v. 6.1 with the GFN2 parameterization, and the GBSA solvation model for dichloromethane.^{8,9} Geometries were refined to meet very tight (vtight) convergence criteria, and the existence of each local minimum was verified by a normal mode frequency calculation. Relaxed potential energy scans were performed with a step of 0.02 Å and a restraining force constant of 10 xTB units.

X-ray crystallography. X-ray quality crystals of **4₂** were grown by vapor fusion, using DCM-toluene mixture as solvent and methanol as antisolvent. Diffraction measurements were performed on a geometry XCALIBUR diffractometer (ω scans), equipped with an ONYX CCD camera, with graphitemonochromatized Cu K α radiation. The data were collected at 100 K, corrected for Lorenz and polarization effects. Data collection, cell refinement, data reduction and analysis were carried out with the Xcalibur PX software, CRYSTALIS CCD and CRYSTALIS RED, respectively (Oxford Diffraction Ltd., Abignon, England, 2009). An analytical absorption correction was applied with the use of CRYSTALIS RED. All structures were solved by direct methods with the SHELXS-97 program and refined using SHELXT-10 with anisotropic thermal parameters for non-H atoms.¹⁰ In the final refinement cycles, all H atoms were treated as riding atoms in geometrically optimized positions. CCDC 1501094 contains the supplementary crystallographic data for this paper. These data can be obtained free of charge from the Cambridge Crystallographic Data Centre via www.ccdc.cam.ac.uk/data_request/cif.

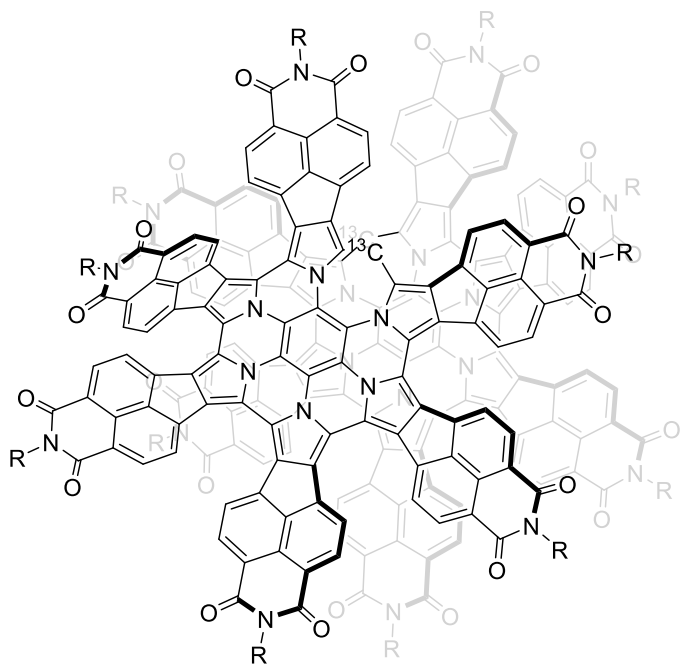
Synthesis



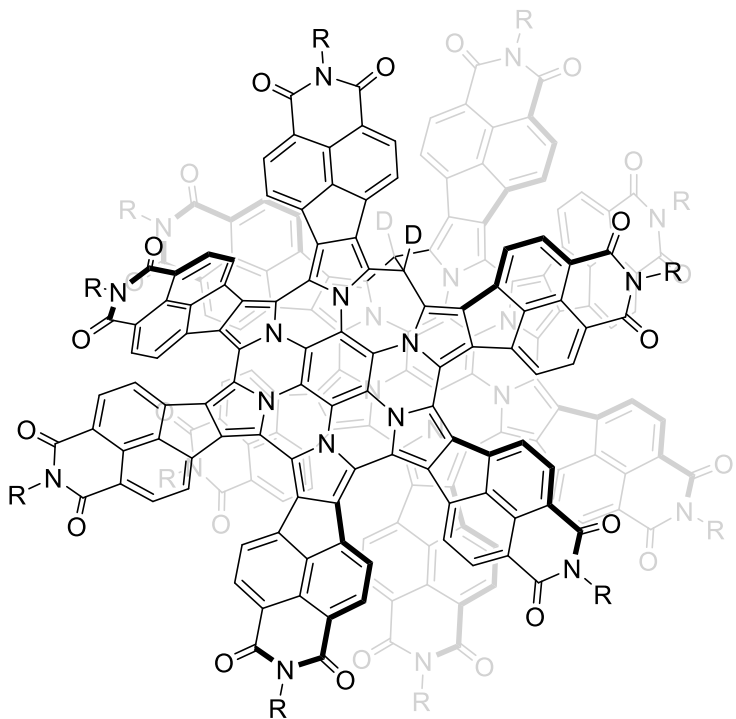
Compound (6). Under an inert atmosphere, **5** (100.0 mg) was dissolved in dichloromethane (10 mL). A 0.5 M oxygen-free solution of FeCl_3 (0.77 mL) in dichloromethane (containing 10% nitromethane) was added. The reaction mixture was stirred at 18 °C for 1 h. After 1 h, the reaction mixture was washed with a 10% solution of KSCN in water (100 mL), water, and a 2% aqueous solution of hydrazine. The organic layer was stripped of solvent and dried under reduced pressure, to yield a dark violet solid (97 mg, 98%). **$^1\text{H NMR}$** (600 MHz, chloroform-*d*, 300 K): δ 8.80–8.72 (8H, m), 8.70 8.61 (4H, m), 8.32 (2H, s), 8.08 (2H, d, 3J = 7.2 Hz), 7.82 (4H, m), 7.77 (2H, d, 3J = 7.4 Hz), 7.69 (2H, d, 3J = 7.6 Hz), 7.59 (2H, d, 3J = 7.5 Hz), 7.48–7.41 (6H, m), 7.38–7.23 (12H, m), 2.95–2.50 (12H, m), 1.28–0.92 (72H, m). **$^{13}\text{C NMR}$** (151 MHz, chloroform-*d*, 300 K): δ 163.8, 163.7, 163.7, 163.7, 145.9, 145.8, 145.7, 145.7, 137.5, 137.5, 137.2, 137.2, 137.0, 137.0, 136.6, 136.6, 136.4, 136.3, 136.2, 136.1, 133.0, 132.9, 132.9, 132.8, 132.7, 130.9, 130.8, 130.8, 129.69, 129.6, 129.4, 129.4, 129.1, 129.1, 128.7, 128.1, 128.0, 127.4, 126.9, 126.9, 126.0, 125.7, 125.7, 125.51, 125.3, 124.2, 124.2, 124.1, 124.0, 121.9, 121.9, 121.8, 121.8, 121.7, 121.7, 121.6, 121.6, 121.5, 121.26, 121.2, 120.6, 117.5, 117.3, 116.2, 116.1, 115.9, 113.2, 110.9, 110.3, 29.3, 29.3, 29.2, 29.2, 29.2, 29.1, 24.1, 24.1, 24.1, 24.0, 24.0. **HRMS** (MALDI–TOF): m/z : [M]⁺ Calcd for $\text{C}_{174}\text{H}_{128}\text{N}_{12}\text{O}_{12}$: 2576.9769; Found 2576.9713. **UV-vis** (dichloromethane, 300 K) λ [nm] (ϵ in $\text{M}^{-1} \text{cm}^{-1}$): 354 (105 800) 370 (108 500), 561 (67 300), 610 (50 400).



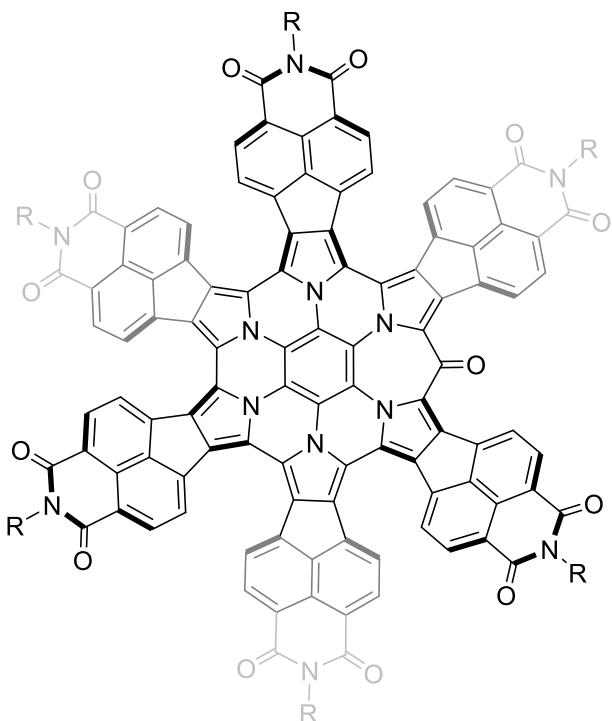
Compound (4₂). In an inert-atmosphere glovebox, a mixture of **6** (70.0 mg, 0.028 mmol), paraformaldehyde (3.3 mg, 0.109 mmol), and camphorsulfonic acid (38.6 mg, 0.163 mmol) was transferred to a pressure tube and dissolved in 150 μ L of chloroform. The tube was sealed, taken out of the glovebox and heated at 90 °C for 17 h. The mixture was diluted with water and extracted with chloroform (50 mL \times 3). Organic fractions were combined and the solvent was removed under reduced pressure. The residue was subjected to column chromatography (grade V alumina, chloroform stabilized with amylene). The pure product was obtained as the third fraction, and isolated as a dark violet solid (49.6 mg, 70%). **¹H NMR** (600 MHz, chloroform-d, 300 K): δ 9.03 (2H, d, ³J = 7.7 Hz), 8.93 (2H, d, ³J = 7.7 Hz), 8.83 (4H, m), 8.75 (2H, d, ³J = 7.7 Hz), 8.64 (4H, m), 8.36 (2H, d, ³J = 7.4 Hz), 8.31 (2H, d, ³J = 7.4 Hz), 8.27 (2H, d, ³J = 7.3 Hz), 8.06 (4H, m), 7.99 (2H, d, ³J = 7.2 Hz), 7.74 (2H, d, ³J = 7.7 Hz), 7.65 (4H, m), 7.57-7.34 (32H, m), 7.33-7.25 (6H, m), 7.23-7.18 (6H, m), 7.15 (2H, d, ³J = 7.6 Hz), 7.11 (2H, d, ³J = 7.2 Hz), 7.00 (2H, d, ³J = 7.6 Hz), 6.92-6.87 (4H, m), 3.11 (2H, m), 3.03 (2H, m), 2.91-2.79 (8H, m), 2.75-2.61 (6H, m), 2.47 (4H, m), 2.14 (2H, m), 1.45-0.89 (132H, m), 0.48 (12H, m). **¹³C NMR** (151 MHz, chloroform-d, 300 K): δ 163.4, 163.3, 163.2, 163.2, 163.0, 162.7, 162.5, 162.1, 146.5, 146.4, 146.1, 146.0, 145.8, 145.6, 145.6, 145.5, 145.4, 145.4, 145.4, 145.2, 144.6, 137.5, 137.4, 137.3, 136.7, 136.5, 135.5, 135.1, 135.1, 135.1, 134.9, 134.7, 134.5, 134.4, 134.3, 133.7, 133.5, 133.4, 132.8, 132.7, 132.5, 132.4, 131.6, 130.9, 130.9, 130.8, 130.8, 130.4, 130.2, 130.2, 130.0, 129.8, 129.7, 129.5, 129.3, 129.1, 128.3, 128.0, 127.9, 127.8, 127.6, 127.3, 127.2, 127.1, 126.8, 126.8, 126.7, 126.6, 126.4, 126.3, 126.1, 125.7, 124.9, 124.6, 124.3, 124.28, 124.2, 124.0, 123.9, 123.8, 123.6, 123.1, 123.0, 122.8, 122.7, 122.6, 122.5, 122.4, 122.0, 121.7, 121.6, 121.5, 121.4, 121.2, 120.3, 119.7, 117.0, 116.9, 116.9, 116.1, 116.2, 115.9, 114.8, 114.5, 113.6, 112.3, 112.1, 111.2, 111.1, 47.97, 37.5, 37.5, 37.4, 37.1, 32.8, 31.9, 29.7, 29.7, 29.4, 28.0, 27.1, 26.8, 24.4, 24.3, 24.2, 24.1, 25.0, 25.0, 22.7, 19.8, 14.1. **HRMS** (MALDI-TOF): *m/z*: [M]⁺ Calcd for C₃₅₀H₂₅₄N₂₄O₂₄: 5176.94197; Found 5176.9596. **UV-vis** (Dichloromethane, 300 K) λ [nm] (ϵ in M⁻¹ cm⁻¹): 340 (226 300), 565 (167 400), 600 (160 400).



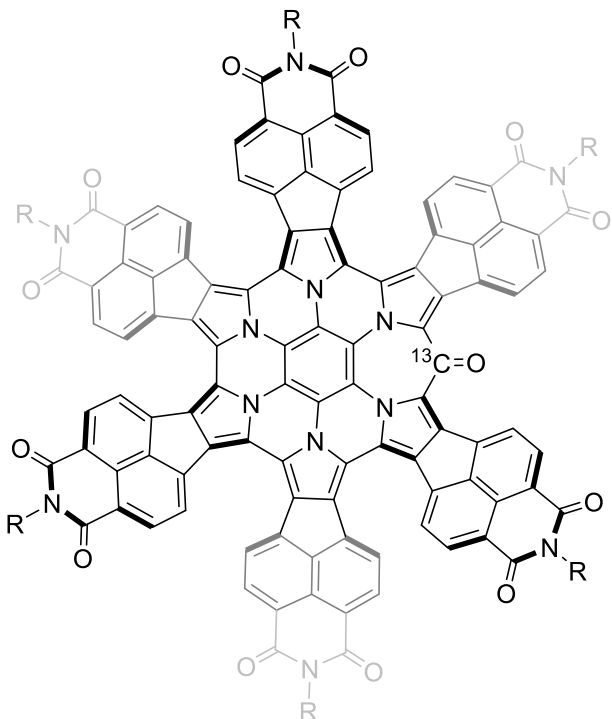
Compound (4₂-c₂**)**. The procedure followed that given for **4₂**, using **6** (70.0 mg, 0.028 mmol), ¹³C-labeled paraformaldehyde (3.4 mg, 0.109 mmol) and camphorsulfonic acid (38.6 mg, 0.163 mmol). Yield: 54.9 mg (74%). **¹H NMR** (600 MHz, chloroform-d, 300 K): δ 9.03 (2H, d, ³J = 7.7 Hz), 8.93 (2H, d, ³J = 7.7 Hz), 8.83 (4H, m), 8.75 (2H, d, ³J = 7.7 Hz), 8.64 (4H, m), 8.36 (2H, d, ³J = 7.4 Hz), 8.31 (2H, d, ³J = 7.4 Hz), 8.27 (2H, d, ³J = 7.3 Hz), 8.06 (4H, m), 7.98 (2H, d, ³J = 7.2 Hz), 7.75 (2H, d, ³J = 7.7 Hz), 7.65 (4H, m), 7.57-7.25 (38H, m), 7.23-7.18 (6H, m), 7.15 (2H, d, ³J = 7.6 Hz), 7.11 (2H, d, ³J = 7.2 Hz), 7.00 (2H, d, ³J = 7.6 Hz), 6.92-6.67 (4H, m), 3.11 (2H, m), 3.03 (2H, m), 2.91-2.79 (8H, m), 2.75-2.61 (6H, m), 2.47 (4H, m), 2.14 (2H, m), 1.45-0.89 (132H, m), 0.48 (12H, m). **¹³C NMR** (151 MHz, chloroform-d , 300 K): δ 163.4, 163.3, 163.2, 163.2, 163.0, 162.7, 162.5, 162.1, 146.5, 146.4, 146.1, 146.0, 145.8, 145.6, 145.6, 145.5, 145.4, 145.4, 145.2, 144.6, 137.5, 137.4, 137.3, 136.7, 136.5, 135.5, 135.1, 135.1, 135.1, 134.9, 134.7, 134.5, 134.4, 134.3, 133.7, 133.5, 133.4, 132.8, 132.7, 132.5, 132.4, 131.6, 130.9, 130.9, 130.8, 130.8, 130.4, 130.2, 130.2, 130.0, 129.8, 129.7, 129.5, 129.3, 129.1, 128.3, 128.0, 127.9, 127.8, 127.6, 127.3, 127.2, 127.1, 126.8, 126.8, 126.7, 126.6, 126.4, 126.3, 126.1, 125.7, 124.9, 124.6, 124.3, 124.28, 124.2, 124.0, 123.9, 123.8, 123.6, 123.1, 123.0, 122.8, 122.7, 122.6, 122.5, 122.4, 122.0, 121.7, 121.6, 121.5, 121.4, 121.2, 120.3, 119.7, 117.0, 116.9, 116.9, 116.1, 116.2, 115.9, 114.8, 114.5, 113.6, 112.3, 112.1, 111.2, 111.1, 47.97, 37.5, 37.5, 37.4, 37.1, 32.8, 31.9, 29.7, 29.7, 29.4, 28.0, 27.1, 26.8, 24.4, 24.3, 24.2, 24.1, 25.0, 25.0, 22.7, 19.8, 14.1. **HRMS** (MALDI-TOF): *m/z*: [M]⁺ Calcd for C₃₄₈¹³C₂H₂₅₄N₂₄O₂₄: 5177.94545; Found 5177.9496.



Compound (4_{2-d₂}**).** The procedure followed that given for **4₂**, using **6** (30.0 mg, 0.012 mmol), deuterated paraformaldehyde (1.8 mg, 0.059 mmol) and camphorsulfonic acid-*d* (18.9 mg, 0.084 mmol) in 75 μ L of chloroform. Yield: 20.7 mg (67%). **¹H NMR** (600 MHz, chloroform-*d*, 300 K): δ 9.03 (2H, d, ³J = 7.7 Hz), 8.93 (2H, d, ³J = 7.7 Hz), 8.83 (4H, m), 8.75 (2H, d, ³J = 7.7 Hz), 8.64 (4H, m), 8.36 (2H, d, ³J = 7.4 Hz), 8.31 (2H, d, ³J = 7.4 Hz), 8.27 (2H, d, ³J = 7.3 Hz), 8.06 (4H, m), 7.97 (2H, d, ³J = 7.2 Hz), 7.74 (2H, d, ³J = 7.7 Hz), 7.65 (4H, m), 7.57-7.25 (38H, m), 7.23-7.18 (6H, m), 7.15 (2H, d, ³J = 7.6 Hz), 7.11 (2H, d, ³J = 7.2 Hz), 7.00 (2H, d, ³J = 7.6 Hz), 6.89 (2H, d, ³J = 7.4 Hz), 3.11 (2H, m), 3.03 (2H, m), 2.91-2.79 (8H, m), 2.75-2.61 (6H, m), 2.47 (4H, m), 2.14 (2H, m), 1.45-0.89 (132H, m), 0.48 (12H, m). **HRMS** (MALDI-TOF): *m/z*: [(M/2)]⁺ Calcd for (C₃₅₀H₂₅₂D₂N₂₄O₂₄)/2: 2588.9754; Found 2588.9973.



Compound (7). **4₂** (6 mg, 1 μ mol) was dissolved in toluene (0.5 mL). The solution was irradiated with a UV lamp. After 0.5 h the solution was exposed to air for additional 12 h. The crude mixture was then purified using column chromatography (grade V alumina, chloroform stabilized with amylene). The pure product was obtained as a green solid (5 mg, 81%). **¹H NMR** (600 MHz, chloroform-*d*₁, 300 K): δ 9.51 (2H, d, ³*J* = 7.2 Hz), 8.91 (2H, d, ³*J* = 7.2 Hz), 8.83-8.72 (6H, m), 8.69 (2H, d, ³*J* = 7.2 Hz), 8.65 (2H, d, ³*J* = 7.4 Hz), 7.84-7.75 (4H, m), 7.61 (2H, d ³*J* = 7.4 Hz), 7.52-7.42 (8H, m) 7.41-7.30 (14H, m), 2.99-2.70 (12H, m), 1.33-1.05 (72H, m). **¹³C NMR** (151 MHz, chloroform-*d*, 300 K): δ 163.7, 163.6, 145.9, 145.8, 145.7, 137.5, 136.9, 136.6, 136.0, 135.5, 134.7, 132.7, 131.8, 130.8, 130.5, 130.1, 129.7, 128.8, 128.1, 127.8, 127.4, 127.3, 126.6, 125.4, 124.3, 124.1, 124.0, 123.9, 122.5, 121.8, 121.7, 117.1, 116.8, 116.7, 116.2, 114.2, 113.3, 107.2, 77.0, 31.9, 29.7, 29.7, 29.6, 29.4, 29.3, 29.3, 29.2, 29.2, 24.1, 24.1, 24.0, 22.7. **HRMS** (MALDI-TOF): *m/z*: [M + Na]⁺ Calcd for C₁₇₅H₁₂₆N₁₂O₁₃: 2609.9510; Found 2609.9719. **UV-vis** (dichloromethane, 300 K) λ [nm] (ϵ in M⁻¹ cm⁻¹): 330 (177 400) 370 (162 600) 570 (101 900) 615 (96 100).



Compound (7-c). Compound **7-c** was prepared using **4₂-c₂** (6.2 mg, 1 μ mol) as the starting material according to the procedure given for **7**, to yield the product as a green solid (5 mg, 79%). **¹H NMR** (600 MHz, chloroform-*d*₁, 300 K): δ 9.51 (2H, d, ³*J* = 7.2 Hz), 8.91 (2H, d, ³*J* = 7.2 Hz), 8.83-8.72 (6H, m), 8.69 (2H, d, ³*J* = 7.2 Hz), 8.65 (2H, d, ³*J* = 7.4 Hz), 7.84-7.75 (4H, m), 7.61 (2H, d ³*J* = 7.4 Hz), 7.53-7.42 (8H, m) 7.41-7.30 (14H, m), 2.99-2.70 (12H, m), 1.33-1.05 (72H, m). **¹³C NMR** (151 MHz, chloroform-*d*, 300 K): δ 163.7, 163.6, 145.9, 145.8, 145.7, 137.5, 136.9, 136.6, 136.0, 135.5, 134.7, 132.7, 131.8, 130.8, 130.5, 130.1, 129.7, 128.8, 128.1, 127.8, 127.4, 127.3, 126.6, 125.4, 124.3, 124.1, 124.0, 123.9, 122.5, 121.8, 121.7, 117.1, 116.8, 116.7, 116.2, 114.2, 113.3, 107.2, 77.0, 31.9, 29.7, 29.7, 29.6, 29.4, 29.3, 29.3, 29.2, 29.2, 24.1, 24.1, 24.0, 22.7.

Additional Figures

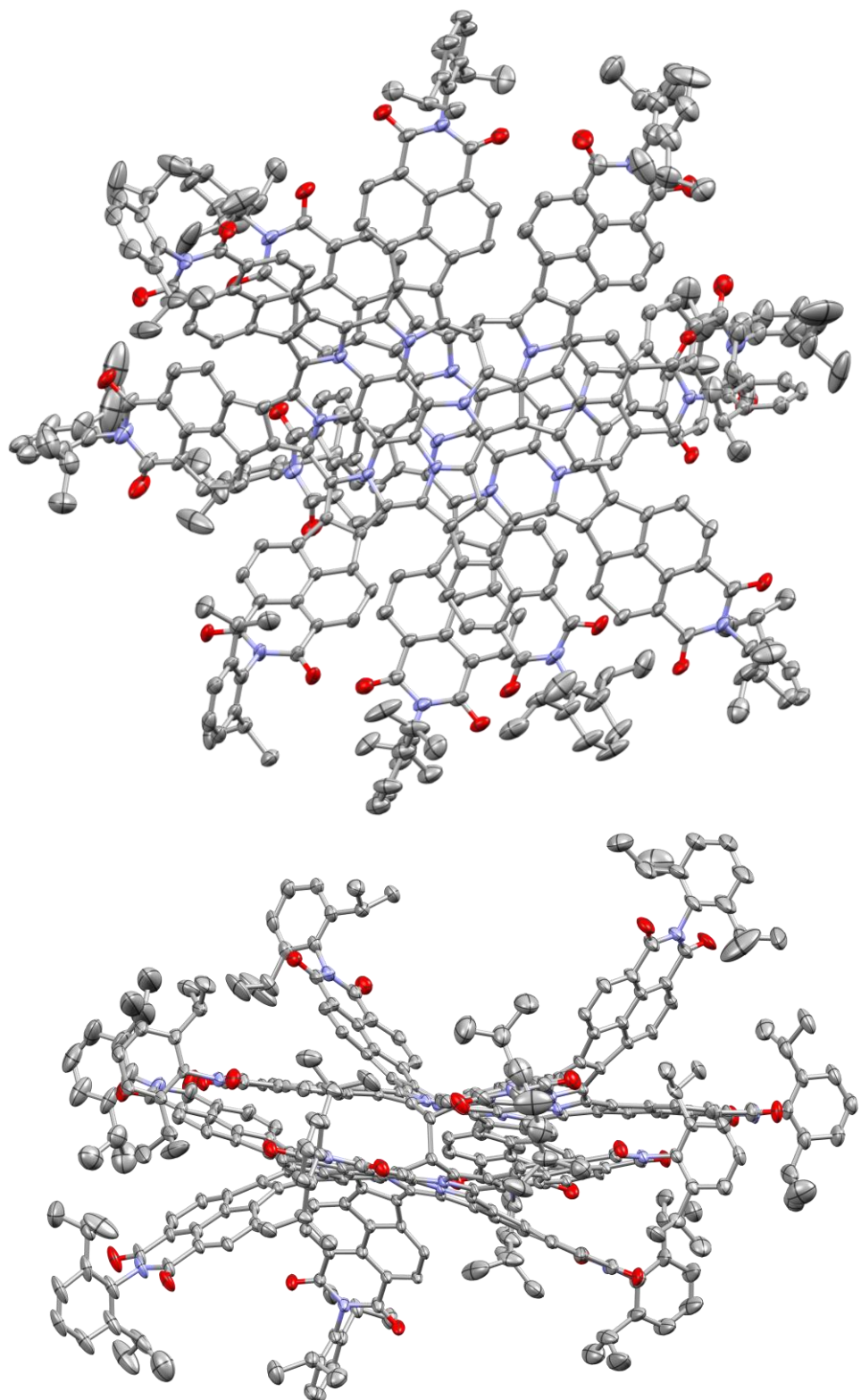


Figure S1. X-ray crystal structure of **4₂**·2(C₇H₈)·43(CH₃OH)·0.65(CH₂Cl₂). Hydrogens and solvents were omitted for clarity.

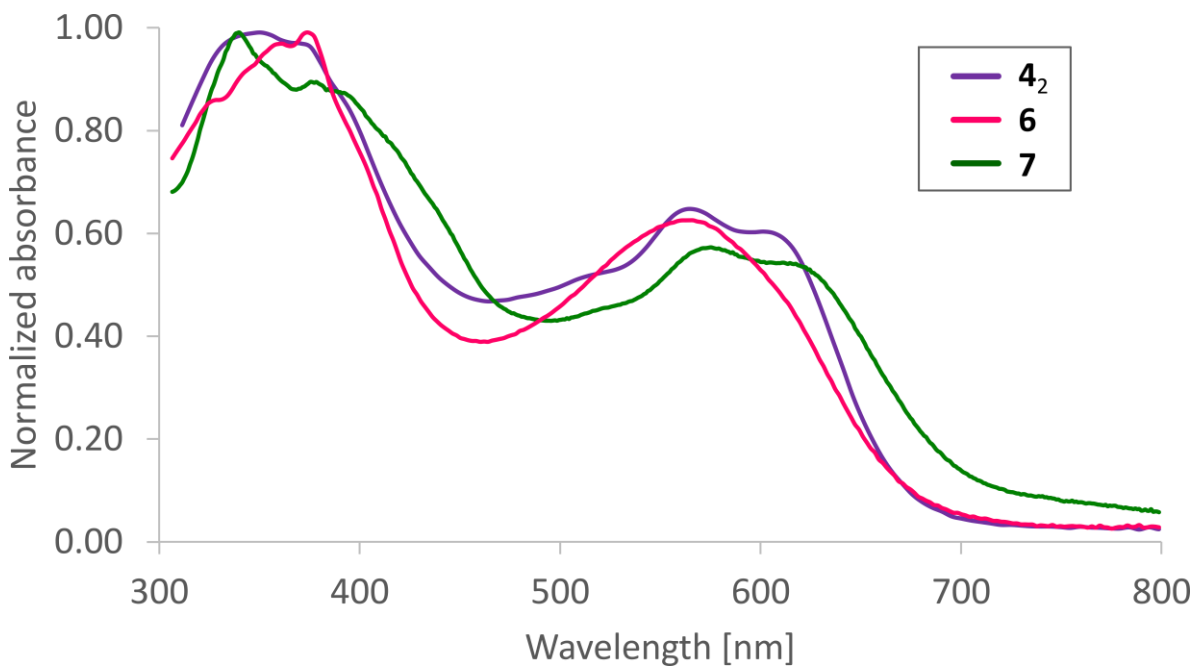


Figure S2. UV-vis absorption spectra of **4₂** (violet), **6** (pink), and **7** (green) in dichloromethane, measured at 293 K.

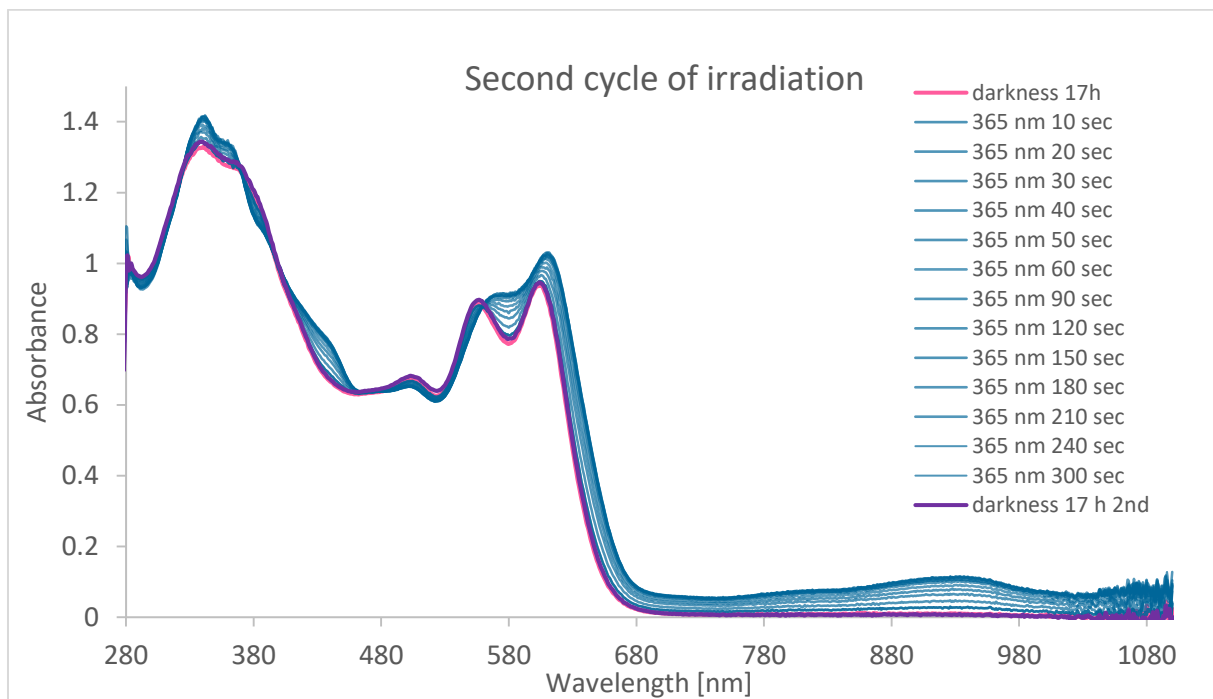


Figure S3. Changes of UV-vis absorption spectra observed for **4₂** during the second cycle of irradiation with a UV lamp (365 nm, in toluene).

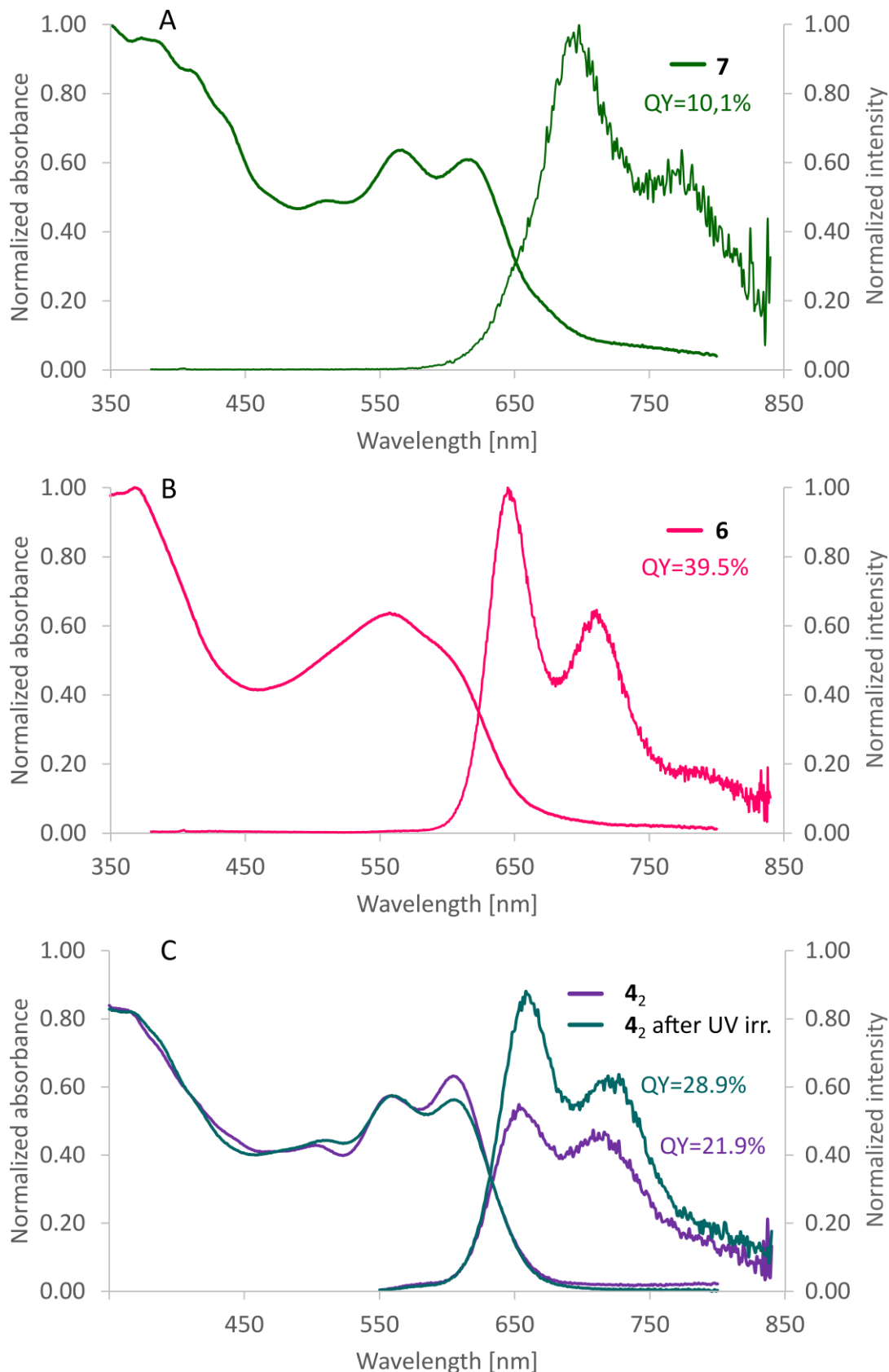


Figure S4. Absorption and emission spectra (toluene, 293 K, excitation at 360 nm). Top: spectra of **7** (A) and **6** (B). Bottom (C): for **4₂** measured before (violet) and after (green) irradiation with UV lamp (at 365 nm) in the presence of atmospheric oxygen: an increase of emission intensity was observed.

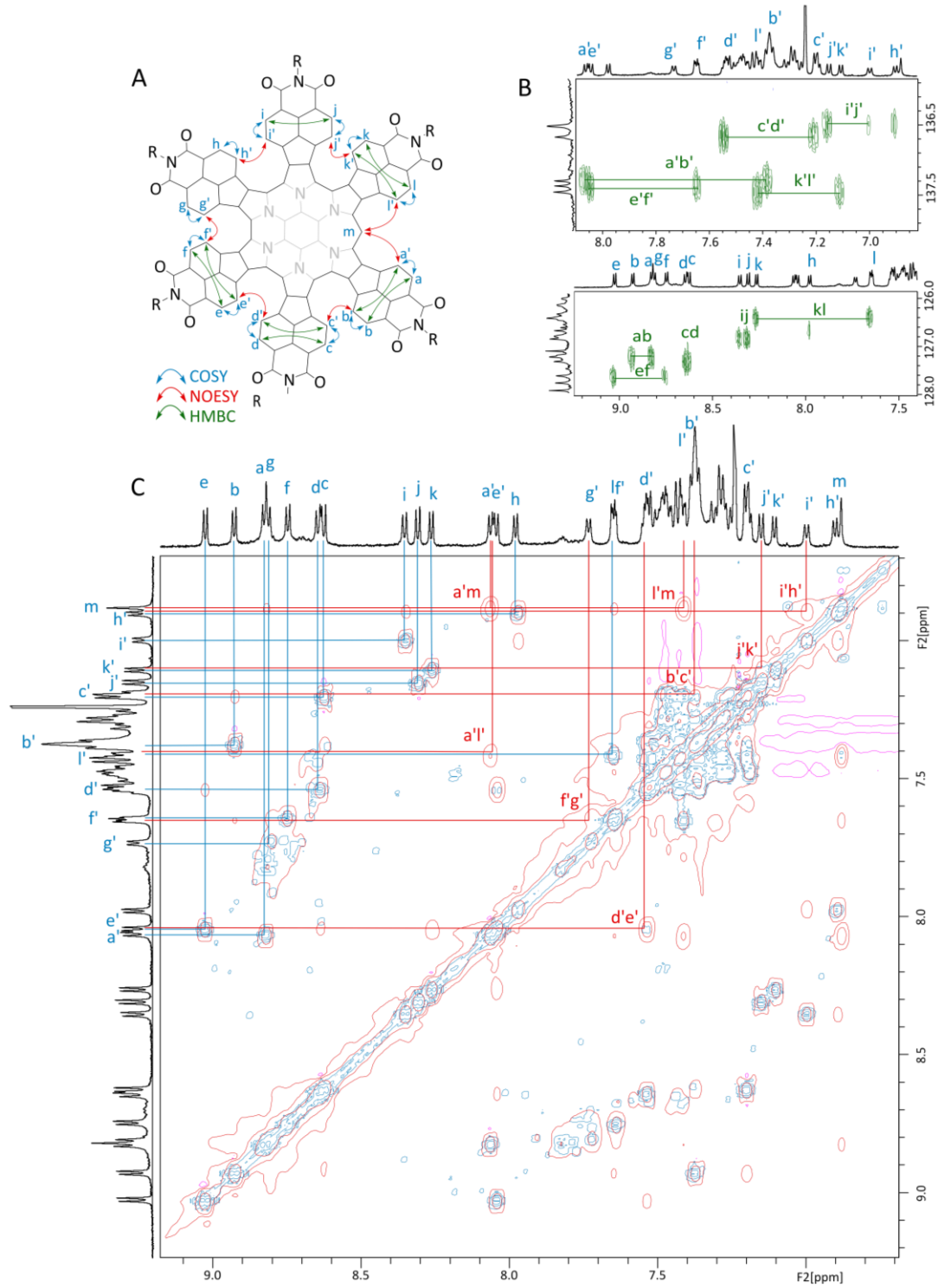


Figure S5. (A) Partial assignment of the ^1H NMR spectrum of **4₂** (chloroform-*d*, 300 K, based on COSY, NOESY, HSQC and HMBC correlations). Blue lines correspond to COSY correlations; red lines correspond to selected EXSY correlations; green lines correspond to HMBC correlations. (B) Selected regions of HMBC correlation spectrum of **4₂**. (C) Overlaid COSY (blue/green) and NOESY (red/pink) correlation spectra recorded for **4₂**. Blue lines show the COSY correlations, red lines show selected NOESY correlations.

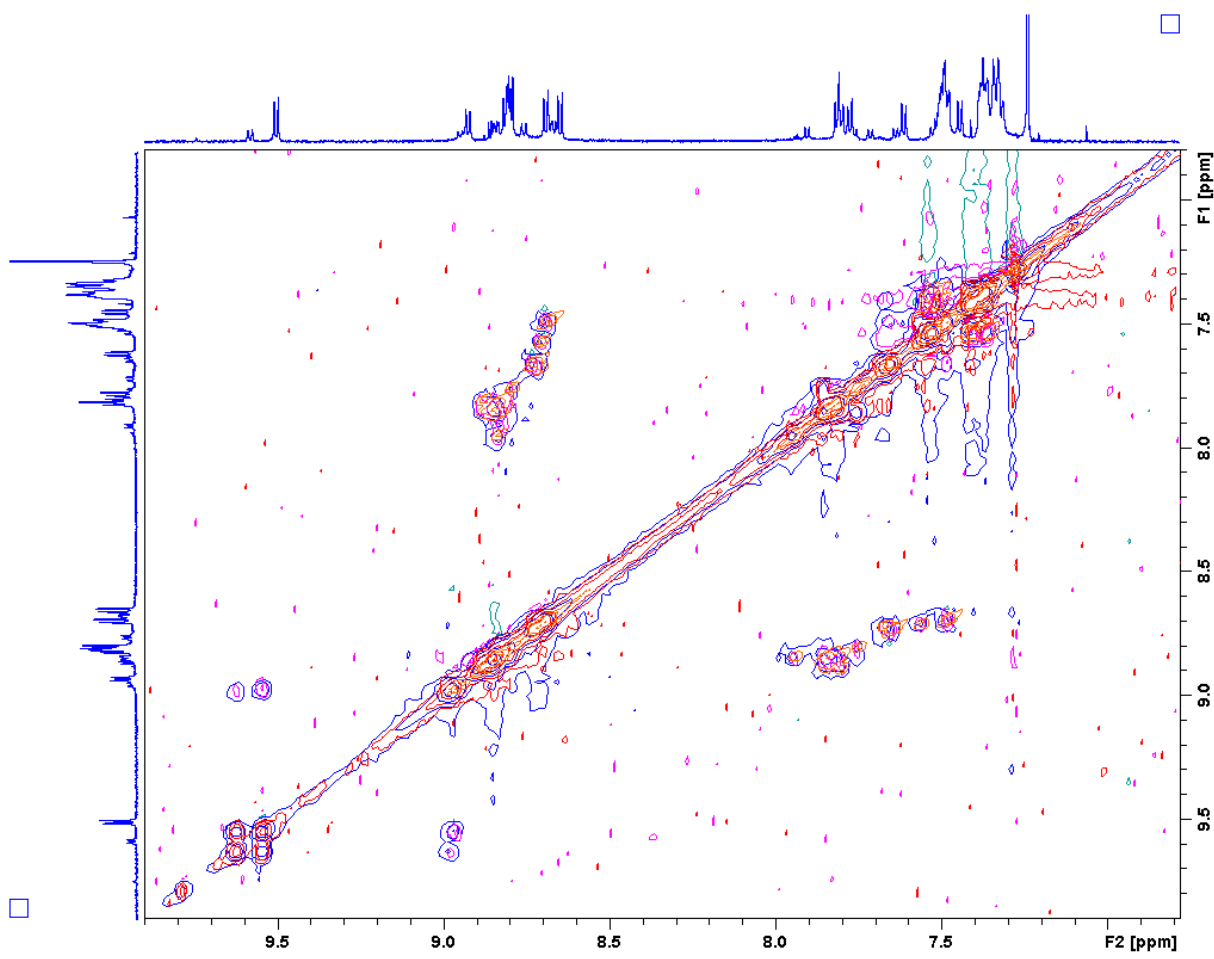


Figure S6. Overlaid selected regions of NOESY (blue/green for positive/negative contours), ROESY (red/pink for positive/negative contours) and COSY (orange) correlation spectra for **7**. EXSY crosspeaks are observable between signals of the two conformers.

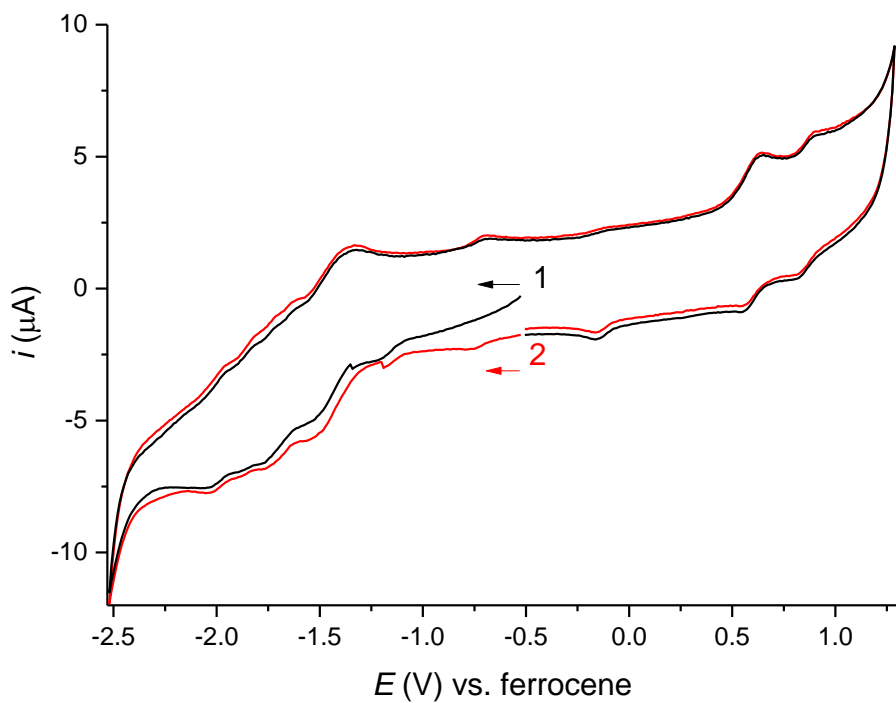


Figure S7. Two consecutive cyclic voltammograms of **4₂** were measured under following conditions: [BuN₄]PF₆ in dichloromethane, scan rate: 100 mV s⁻¹; the voltammograms were referenced with ferrocene/ferrocenium couple as an internal standard.

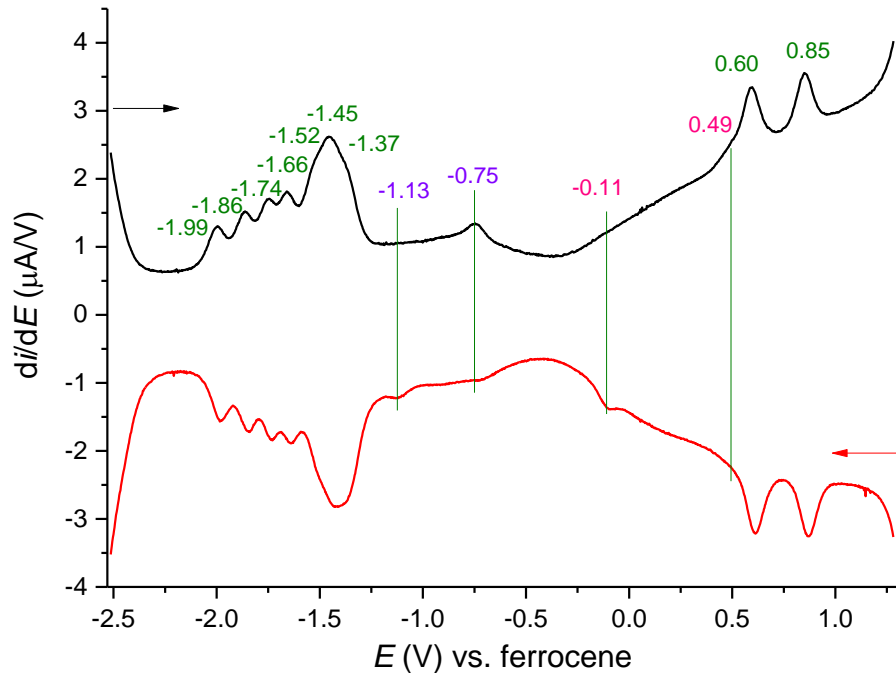


Figure S8. Differential pulse voltammograms of **4₂** in dichloromethane. Directions of the potential scans are indicated with arrows. The number associated with the cathodic scan (black trace) are peak potentials in volts.

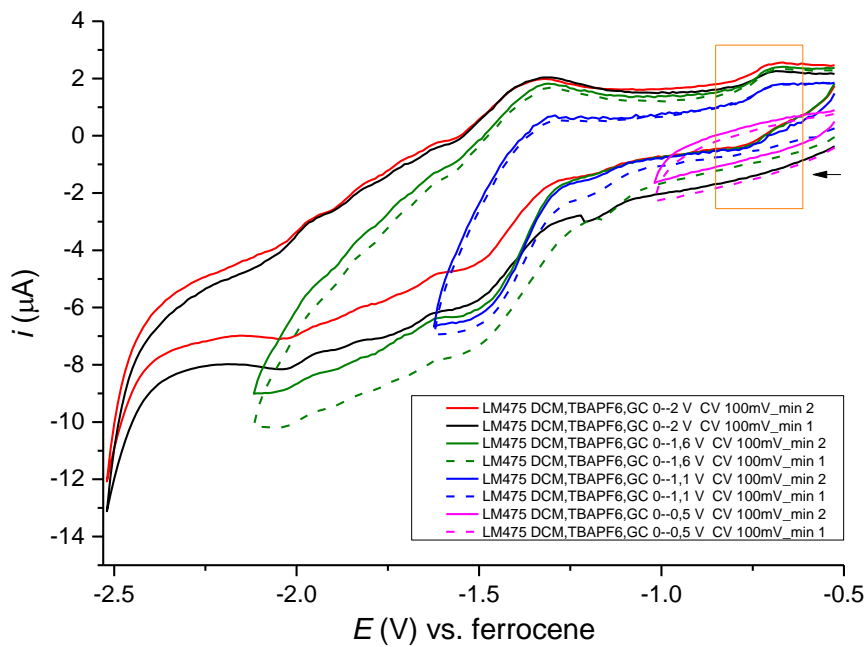


Figure S9. A series of cyclic voltammograms for **4₂** recorded within different reduction potential limits. The orange box indicates a reversible couple at -0.75 V that can be observed after cathodic scan down to -1.6 V.

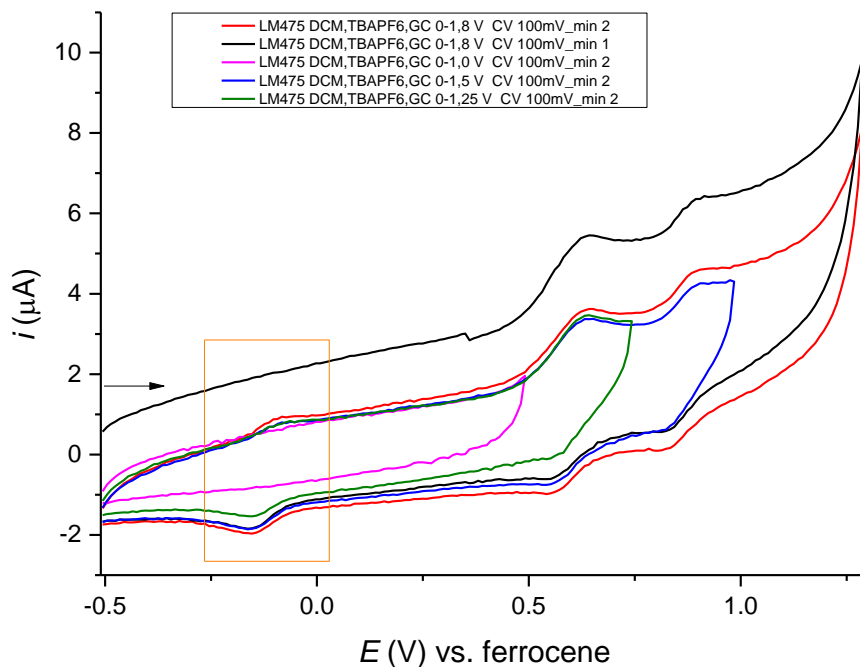


Figure S10. A series of cyclic voltammograms recorded for **4₂** within different oxidation potential limits. The orange box indicates a reversible couple at -0.11 V that can be observed after anodic scan up to 0.6 V.

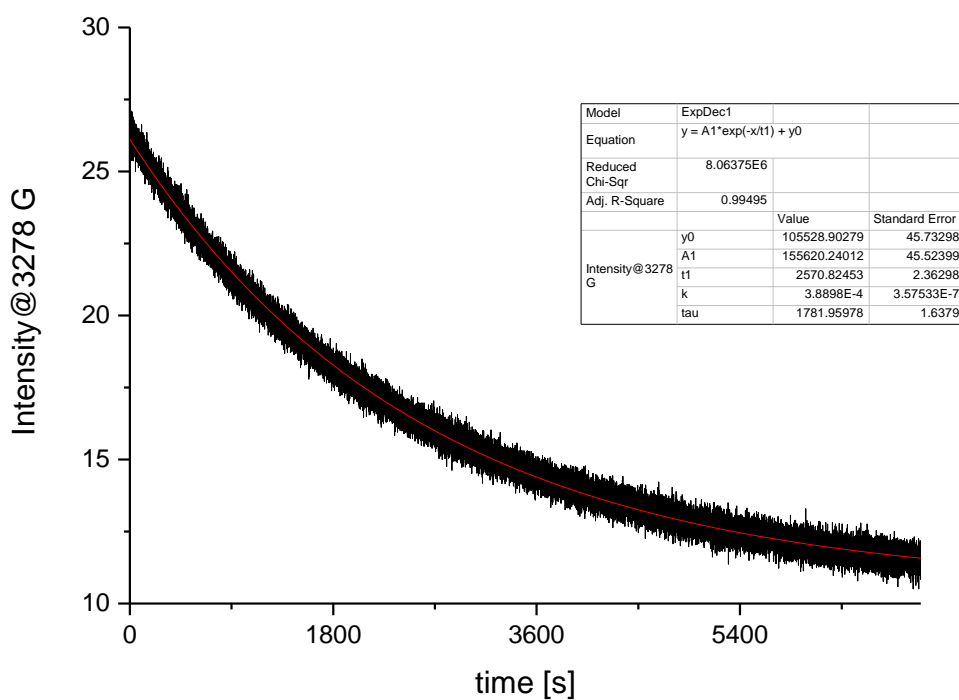
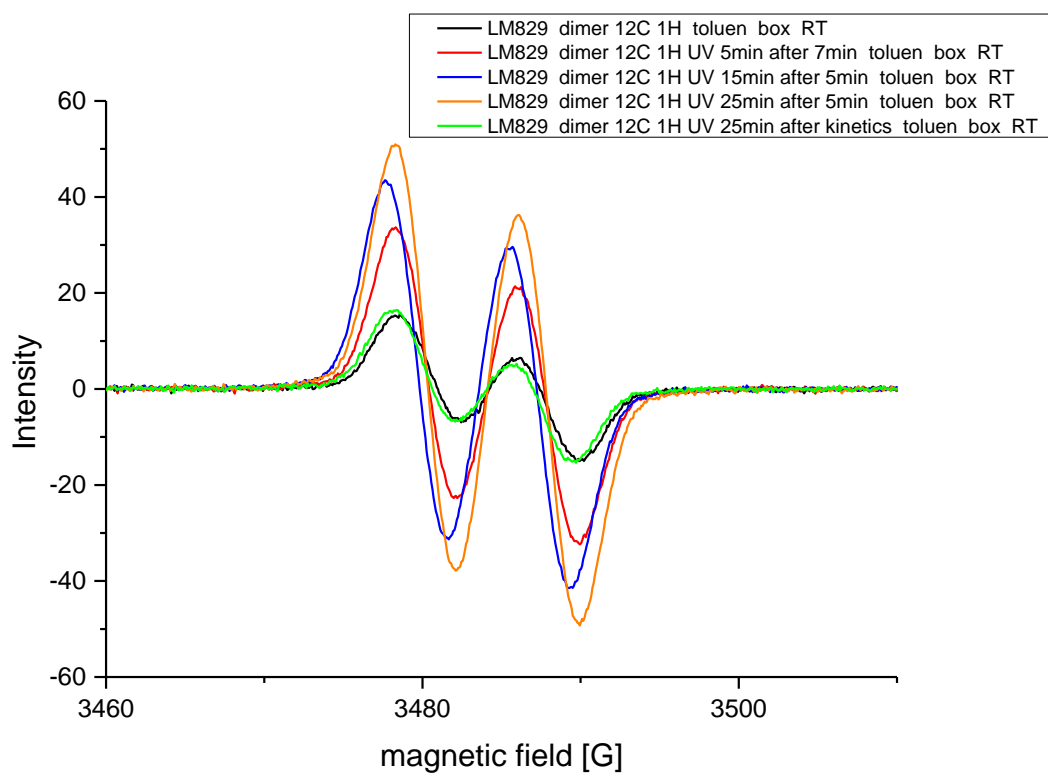


Figure S11. ESR spectra (top) of **4₂**. Bottom: time depended spectrum of intensity at 3275 G (solvent: toluene). The increase of amount of radical after irradiation of the solution with UV (365 nm) and the following decay of radical after protecting the sample from light is observed.

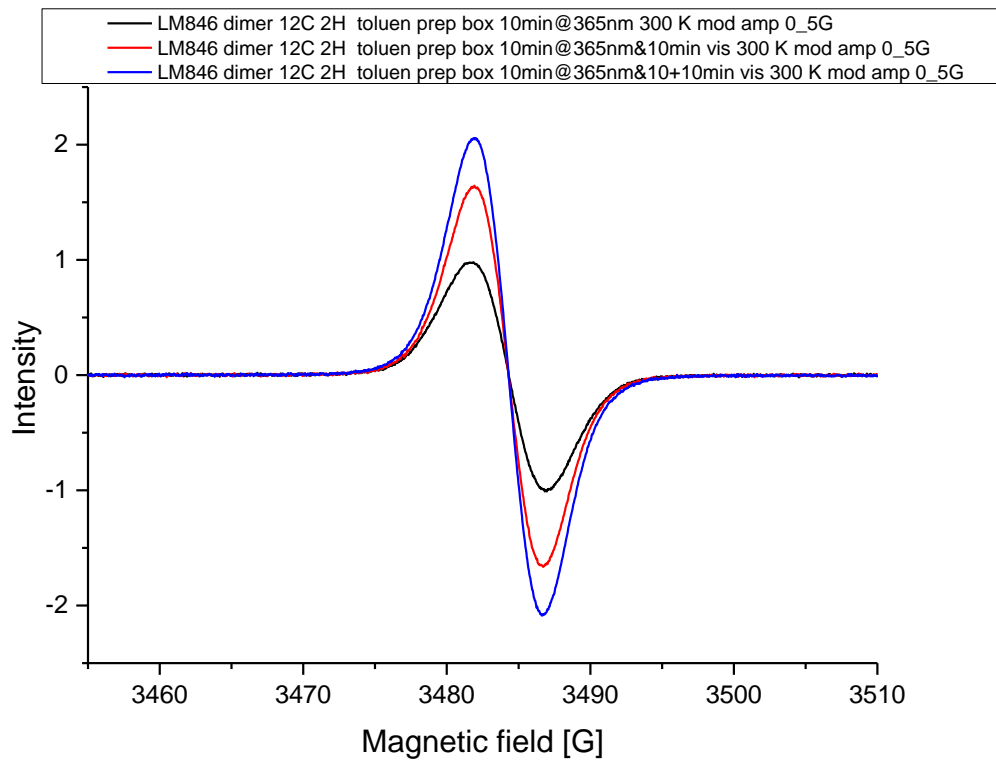


Figure S12. ESR spectra of irradiated toluene solutions of **4₂-d₂**: black line – 10 min irradiation at 365 nm; red line – irradiated for additional 10 min under LED lamp; blue line – irradiated for 10 min under UV light and 20 min LED lamp. The increase of radical is observed after treatment of dimer in toluene solution with different sources of light.

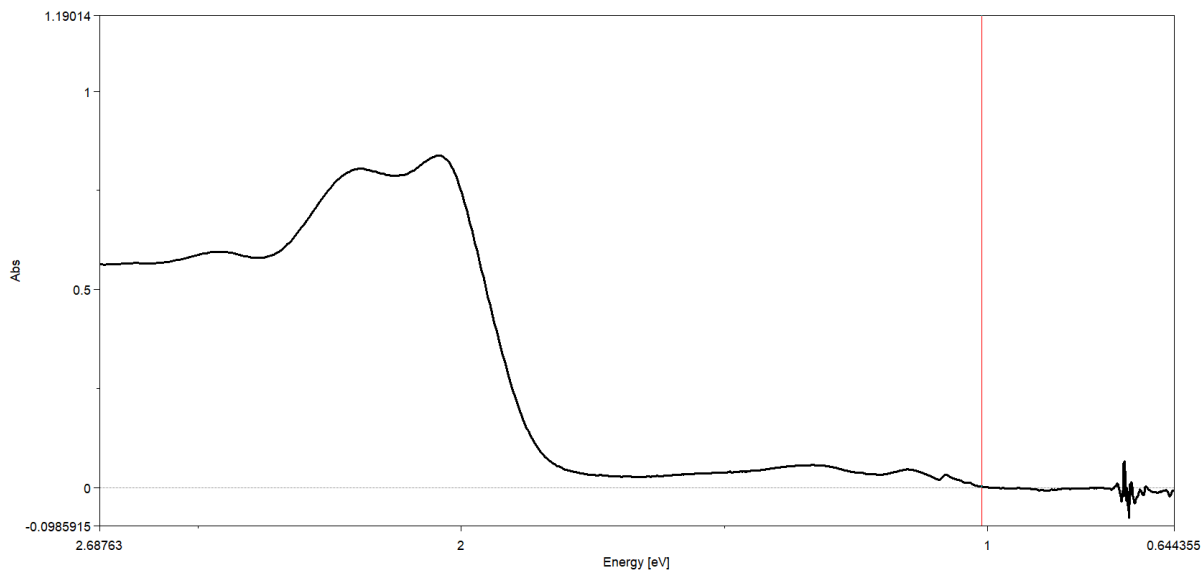


Figure S13. Electronic spectrum of **4°** shown in energy units. The optical bandgap is indicated.

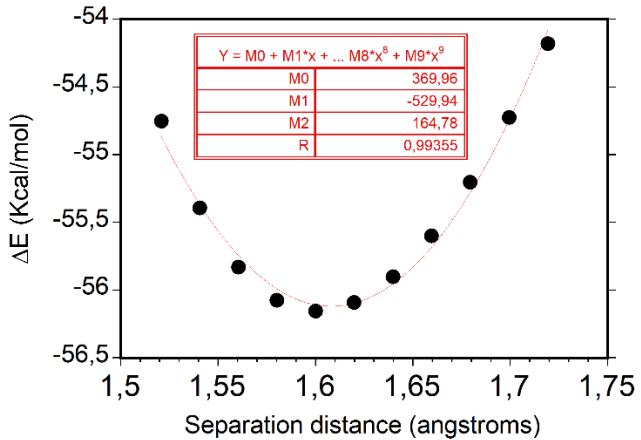


Figure S14. Fitting the ΔE_{SCC} energy (GFN2-xTB) of the $S_0\text{-}\mathbf{4}_2$ PES with a parabolic function. It is assumed that in the vicinity of the $S_0\text{-}\sigma\text{-}\mathbf{4}_2$ minimum, the dominant energy contribution is associated with stretching of the C–C bond. Subject to this assumption, the behavior of ΔE_{SCC} in the proximity of the equilibrium distance will follow harmonic behavior and can be fitted with a parabola, with the factor of the squared term corresponding to half the force constant of the C–C bond. The calculation yields a value of $2.29 \text{ mdyn}\cdot\text{\AA}^{-1}$ (this value increases up to $2.70 \text{ mdyn}\cdot\text{\AA}^{-1}$ when a smaller number of points is used for fitting).

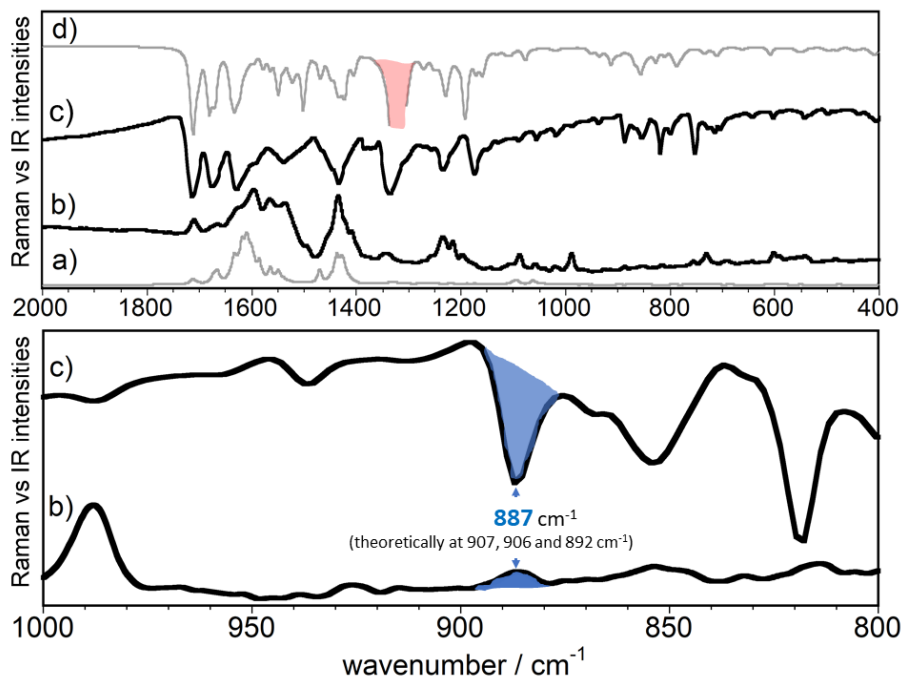


Figure S15. Top: a) Theoretical Raman spectrum of $\mathbf{4}_2$ ($\omega\text{B97XD/3-21G}$); b) 532 nm excitation Raman spectra of $\mathbf{4}_2$, in the solid state at 80 K; c) Fourier-transform infrared spectrum of $\mathbf{4}_2$ in solid state at room temperature; and d) theoretical infrared spectrum of $\mathbf{4}_2$ ($\omega\text{B97XD/3-21G}$). The red shaded highlights the most intense theoretical infrared band which has been partially suppressed to clearly visualize the whole spectrum (see ESI for the complete spectrum and details). Bottom: b) and c) such as the top panel in the inter-fragment C–C stretching mode wavenumber region. The bands shaded in blue correspond to those with associated vibrational modes containing the largest contributions of the inter-fragment C–C stretching mode.

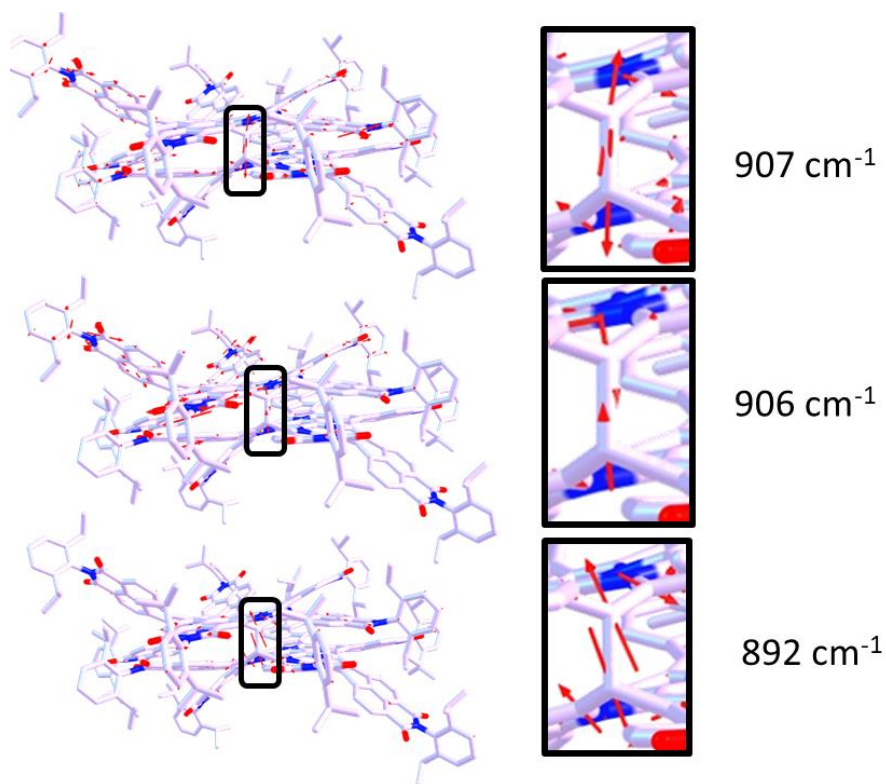


Figure S16. Calculated vibrational eigenvectors associated with the Raman and infrared bands of **4₂** at 907, 906 and 892 cm⁻¹ (ω B97XD/3-21G).

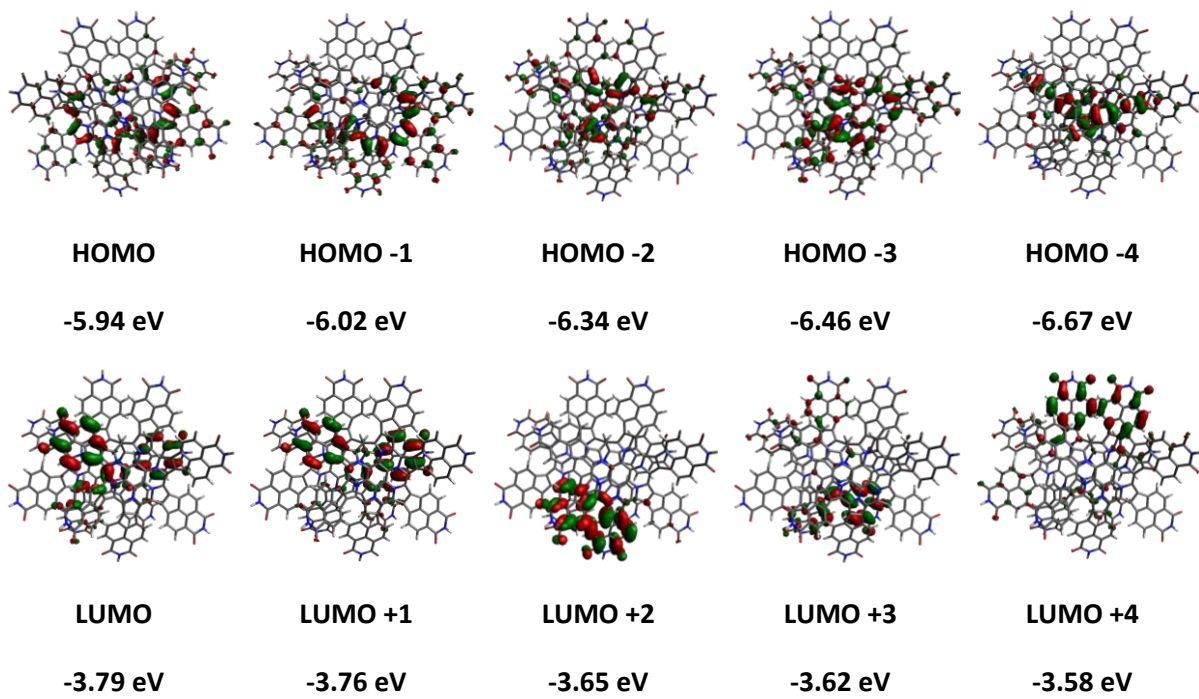


Figure S17. Frontier molecular orbitals (isovalue = 0.02) and orbital energies of **4₂**.

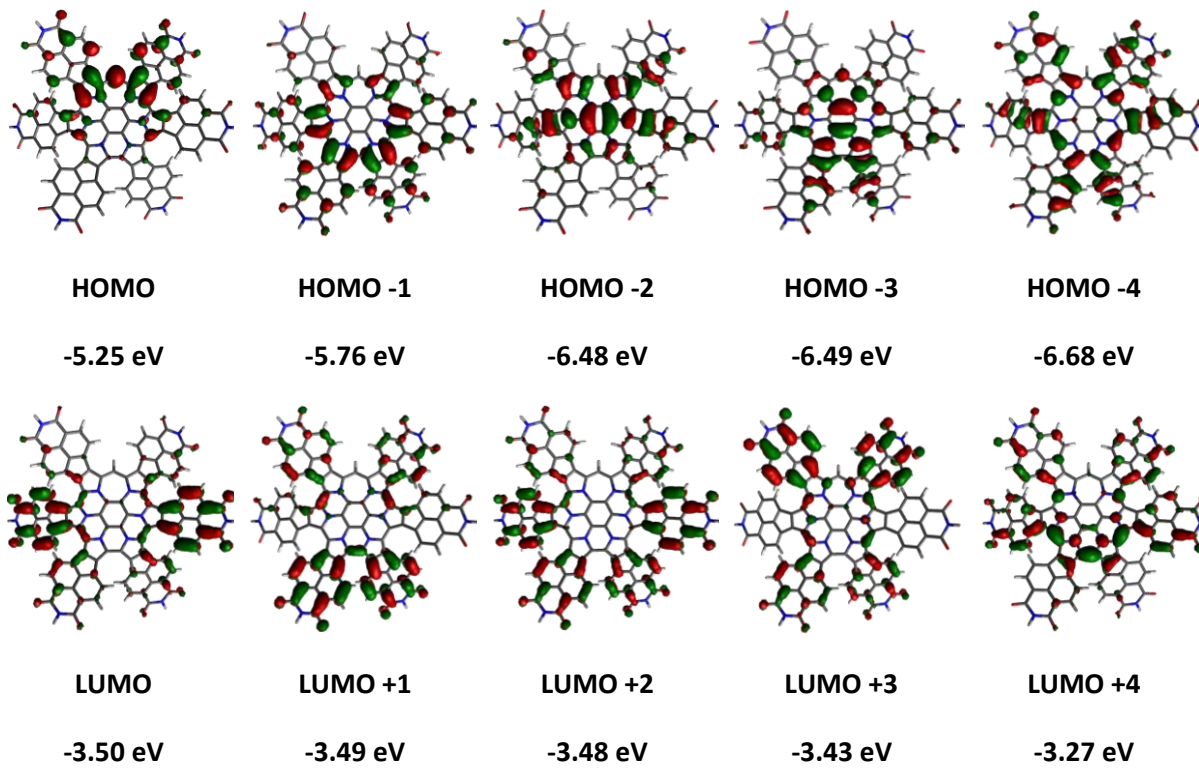
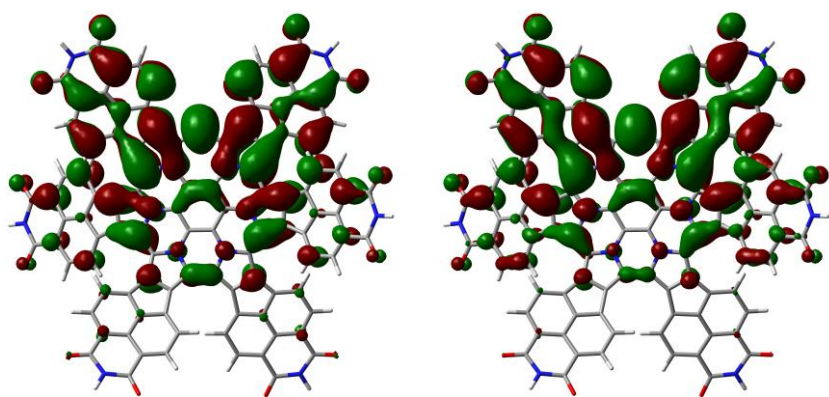


Figure S18. Frontier molecular orbitals (isovalue = 0.02) and orbital energies of **4°**.



Nr orbital	SOMO α -orbital energy	β -LUMO β -orbital energy
418	LUMO +2 -3.48 eV	LUMO +3 -3.42 eV
417	LUMO +1 -3.49 eV	LUMO +2 -3.48 eV
416	LUMO -3.50 eV	LUMO +1 -3.48 eV
415	SOMO -5.25 eV	LUMO -4.12 eV
414	HOMO -1 -5.75 eV	HOMO -5.72 eV
413	HOMO -2 -6.48 eV	HOMO -1 -6.41 eV
412	HOMO -3 -6.49 eV	HOMO -2 -6.45 eV

Figure S19. Frontier molecular α and β orbitals (isovalue = 0.015) and orbital energies of **4 \bullet** .

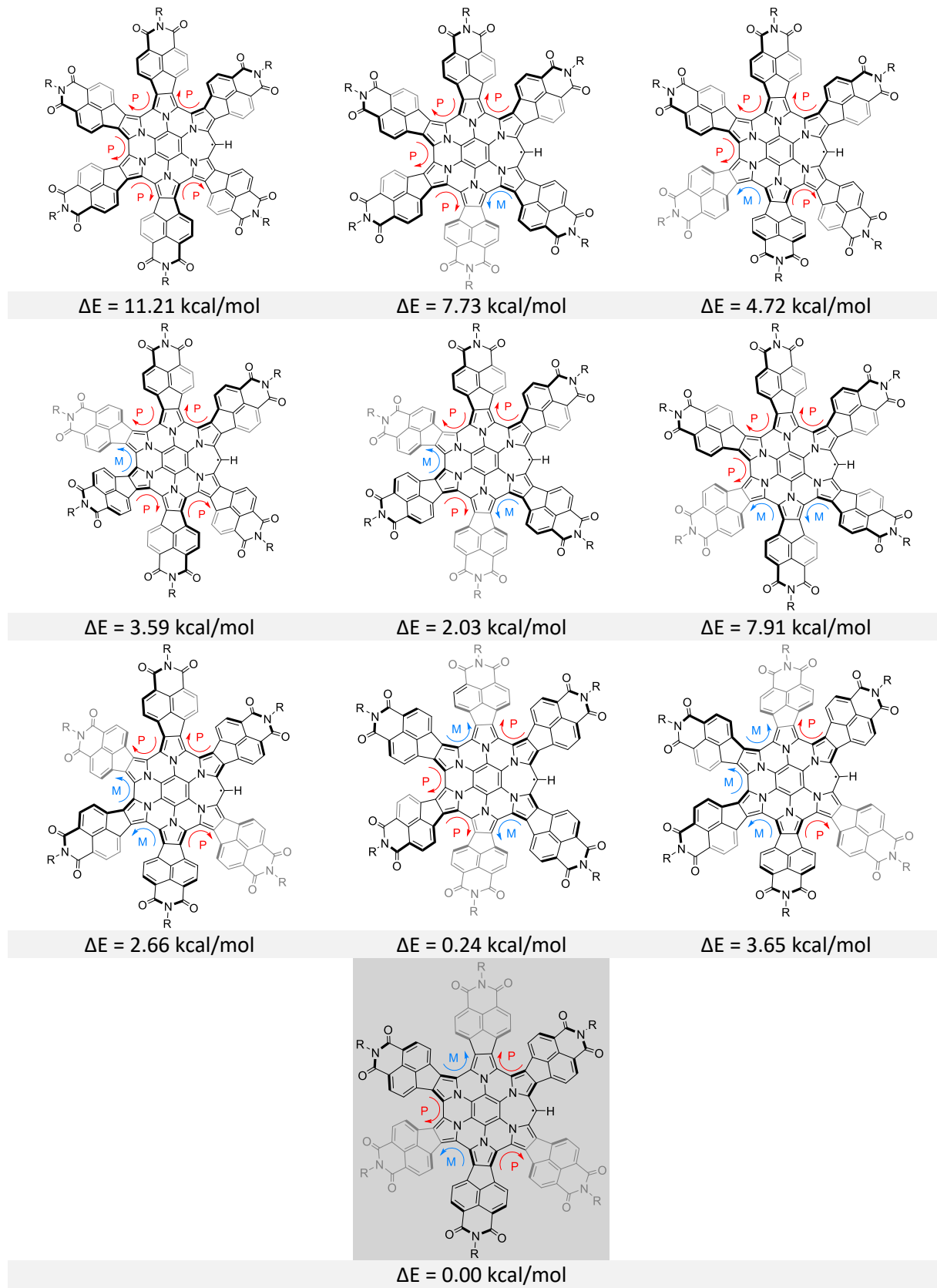


Figure S20. Conformers of **4°** ($\omega\text{B97XD}/6-31g(\text{d},\text{p})$). Energies are given relative to the most stable conformation.

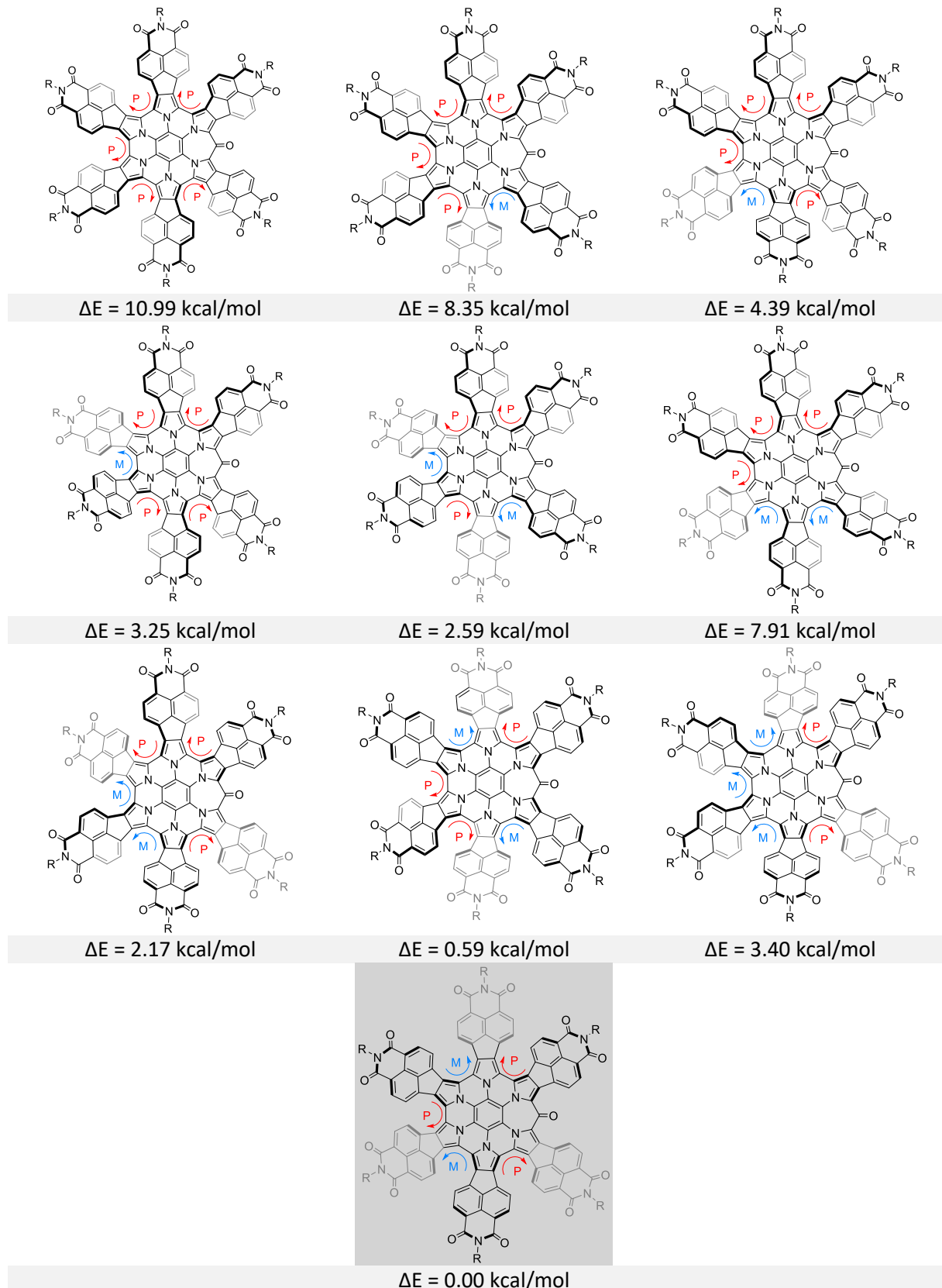


Figure S21. Conformers of **7** ($\omega\text{B97XD}/6-31g(\text{d},\text{p})$). Energies are given relative to the most stable conformation.

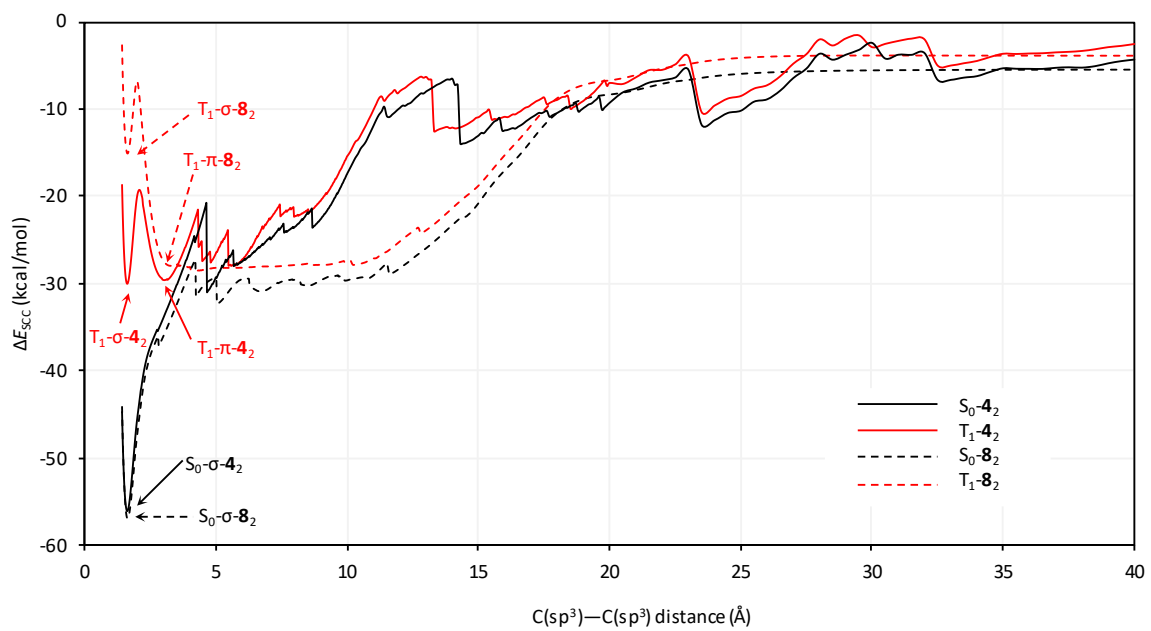


Figure S22. GFN2-xTB relaxed potential energy scans for **4₂** and **8₂** performed along the C(sp³)–C(sp³) bond length coordinate on singlet and triplet hypersurfaces. Energies are given relative to **4[•]** and **8[•]**, respectively.

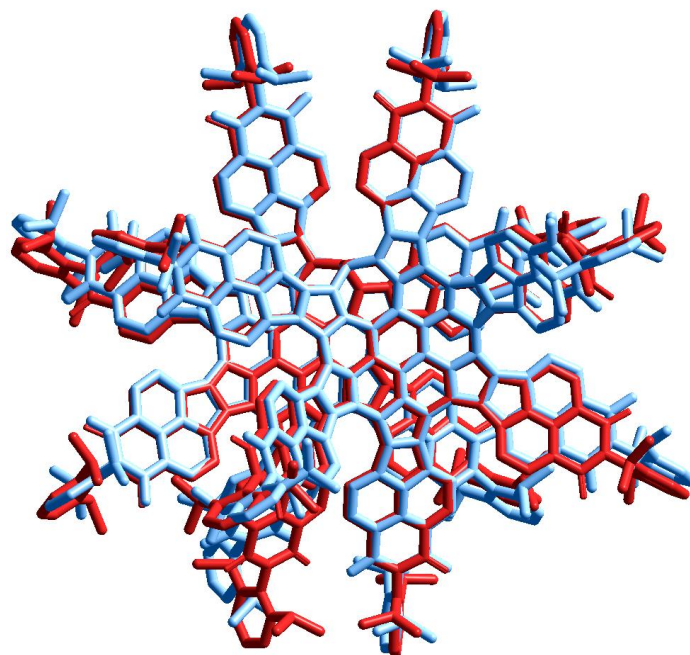


Figure S23. Comparison of the experimental (XRD, blue), and calculated (GFN2-xTB, red) geometries of **4₂**.

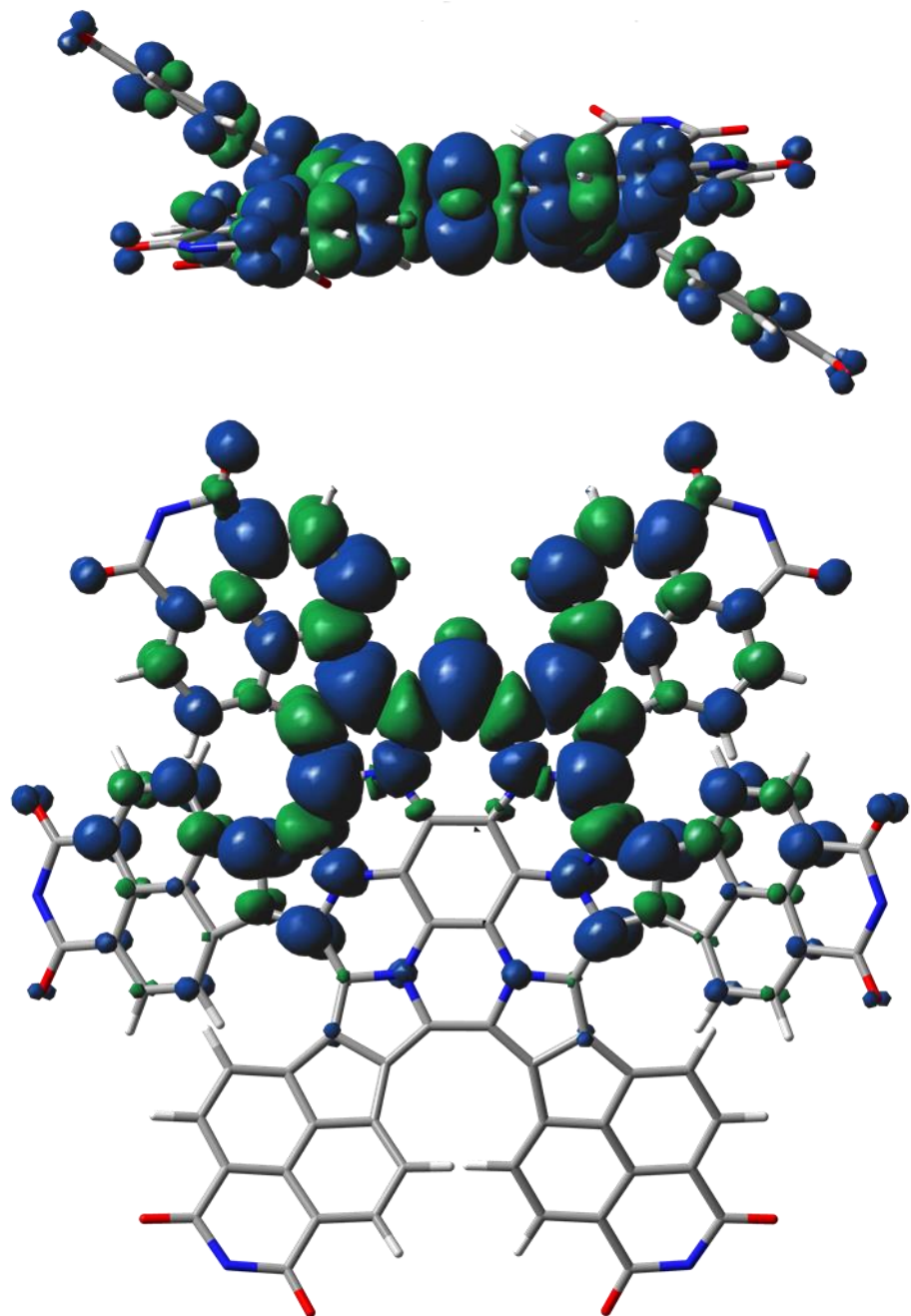


Figure S24. Spin density of monoradical **4*** (ω B97XD/6-31g(d,p), dipp substituents are omitted for clarity).

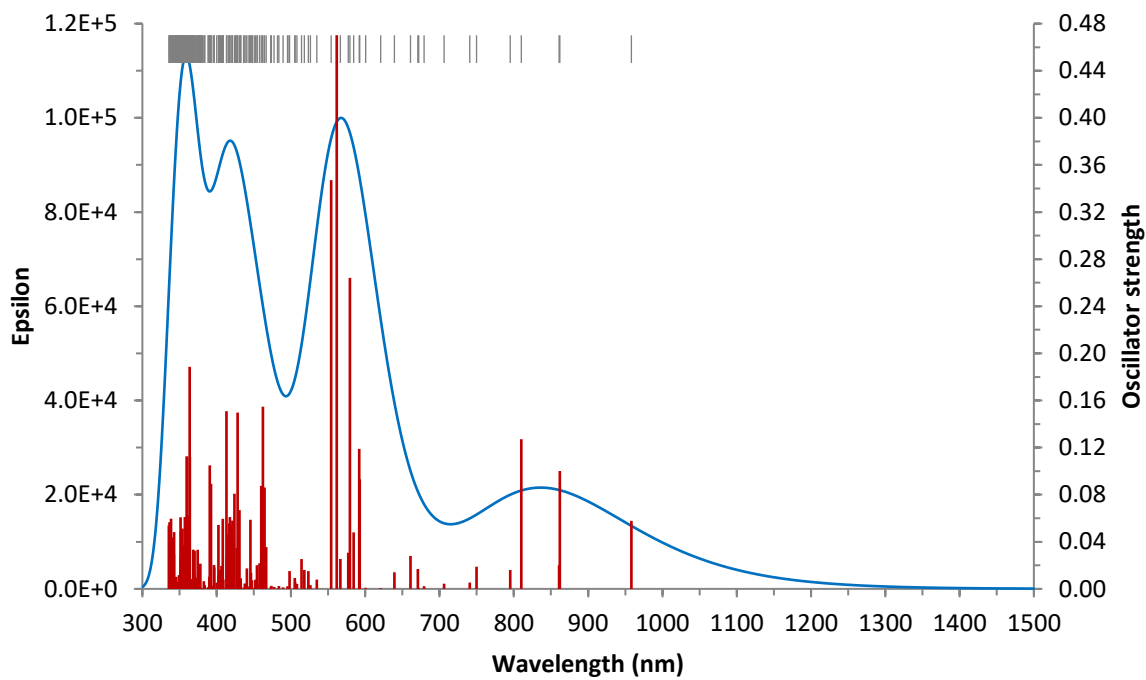


Figure S25. TDA-DFT spectra for **4°** (B3LYP/6-31G(d,p)). Individual transitions are shown as red sticks. The blue envelope is a sum of Gaussian profiles with halfwidths of 1500 cm⁻¹.

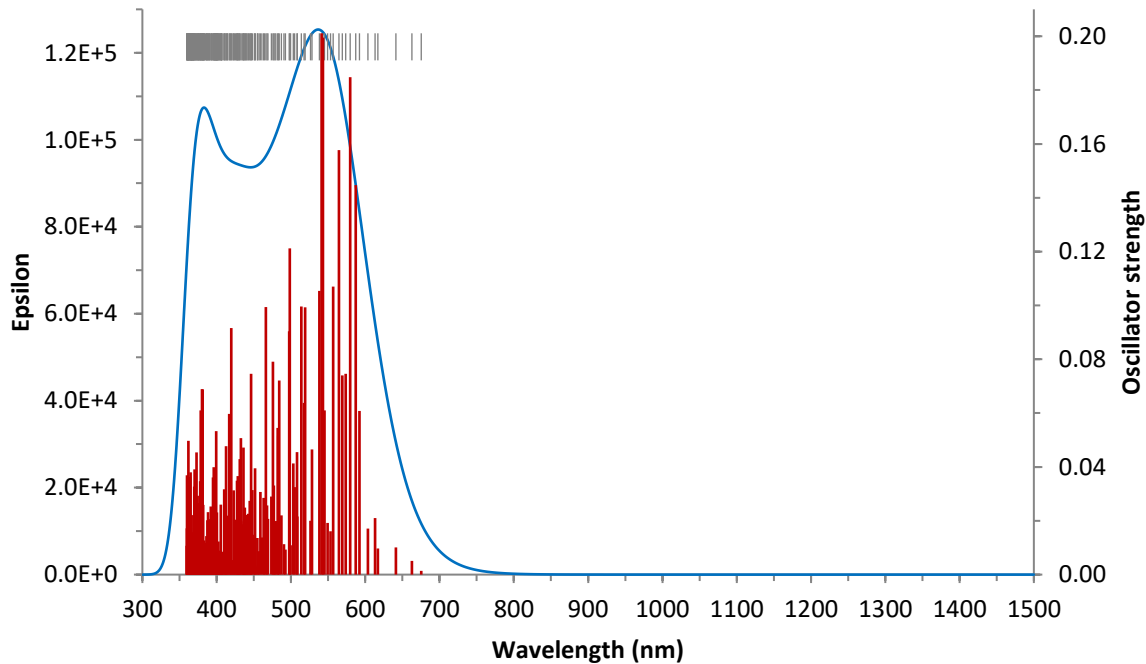


Figure S26. TDA-DFT spectra for **4₂** (B3LYP/3-21g)). Individual transitions are shown as red sticks. The blue envelope is a sum of Gaussian profiles with halfwidths of 1500 cm⁻¹.

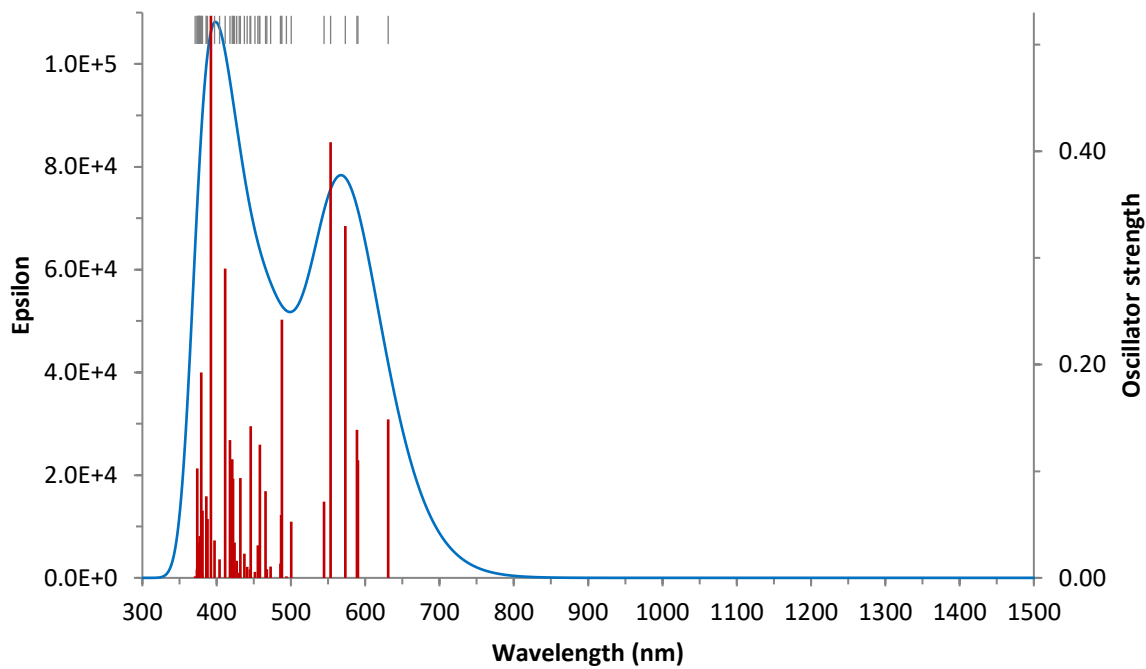


Figure S27. TDA-DFT spectra for **7** (B3LYP/6-31G(d,p)). Individual transitions are shown as red sticks. The blue envelope is a sum of Gaussian profiles with halfwidths of 1500 cm^{-1} .

Additional Tables

Table S1. Energetics of dimerization for **8₂**.

Energy ^[a] (kcal/mol)	S ₀ -σ- 8₂		T ₁ -σ- 8₂		T ₁ -π- 8₂	
	total	ΔE _X ^{def [b]}	ΔE _X ^{int [b]}	total	total	
ΔE _{SCC}	-56.8	40.8	-97.6	-14.5	-27.3	
ΔE _{disp}	-40.5	-0.1	-40.4	-44.0	-42.6	
ΔE _{solv}	7.3	-0.2	7.5	8.3	8.2	
ΔE _{el}	-23.6	41.0	-64.6	2.1	7.1	
ΔG ²⁹⁸	-33.4			5.7	-9.6	
C-C (Å)	1.608			1.612	3.387	
ΔE _{DFT} ^[c]	-64.17					
ΔG ^{298 [c]}	-40.22					
C-C (Å)	1.623					

[a] GFN₂-xTB energies (CH₂Cl₂ solvation) relative to **8^{*}**. ΔE_{el} = ΔE_{SCC} - ΔE_{solv} - ΔE_{disp}, where ΔE_{SCC}, ΔE_{solv}, ΔE_{disp} are respectively the self-consistent charge, solvation, and dispersion energy. [b] Deformation and interaction energy components; X corresponds respectively to SCC, disp, solv, and el.

Table S2. Computational details.

	Code ^[a]	level of theory ^[b]	E ^[c] a.u.	ZPV ^[d] a.u.	lowest freq. ^[e] cm ⁻¹	G ^[f] a.u.
4₂	S_sigma_4_2_DFT	ωB97XD/3-21G	-16514.657313	5.338014	5.26	-16509.674944
	S_sigma_4_2_xTB	GFN2	-1048.958800	5.058700	4.59	-1044.241641
	T_sigma_4_2_xTB	GFN2	-1048.917619	5.052335	2.86	-1044.207578
	T_pi_4_2_xTB	GFN2	-1048.916451	5.052340	2.56	-1044.208757
4[*]	4(.)_DFT	ωB97XD/6-31G(d,p)	-8302.918368	2.628711	4.33	-8300.509367
	4(.)_xTB	GFN2	-524.435060	2.523299	4.02	-522.104235
7	7_DFT	ωB97XD/6-31G(d,p)	-8377.534900	2.624053	4.62	-8375.129916
8₂	S_sigma_8_2_xTB	GFN2	-181.669140	0.720064	10.75	-181.016787
	T_sigma_8_2_xTB	GFN2	-181.601689	0.714514	19.35	-180.954506
	T_pi_8_2_xTB	GFN2	-181.622041	0.713278	7.33	-180.978939
8[*]	8(.)_xTB	GFN2	-90.789276	0.355564	46.06	-90.481810

[a] Geometries available as *.pdb files. [b] CH₂Cl₂ solvation included in all xTB calculations. [c] E_{SCC} and E_{SCF} for xTB and DFT calculations, respectively. [d] zero-point vibrational energy. [e] lowest vibrational frequency. [f] Gibbs free energy.

Table S3. Electronic transitions calculated for **4^{*}** using the TDA/B3LYP/6-31G(d,p) level of theory.

No.	Energy (cm ⁻¹)	λ (nm)	f ^[a]	Major excitations ^[b]			
1	10436	958.2	0.058	HOMO(B)»LUMO(B) (87%)	28	19447	514.2 0.025 H-2(A)»L+2(A) (19%) H-2(B)»L+3(B) (17%)
2	11602	861.9	0.100	HOMO(A)»L+2(A) (75%)	29	19683	508.0 0.004 HOMO(A)»L+7(A) (10%) HOMO(B)»L+6(B) (14%)
3	11615	860.9	0.020	HOMO(A)»LUMO(A) (47%) HOMO(A)»L+3(A) (39%)	30	19779	505.6 0.006 H-6(B)»LUMO(B) (14%)
4	12345	810.0	0.127	HOMO(A)»LUMO(A) (35%) HOMO(A)»L+3(A) (41%)	31	19796	505.2 0.009 H-5(B)»LUMO(B) (10%) HOMO(B)»L+6(B) (15%)
5	12577	795.1	0.016	HOMO(A)»L+1(A) (57%) HOMO(A)»L+4(A) (11%)	32	20077	498.1 0.015 H-1(A)»L+5(A) (48%) HOMO(B)»L+6(B) (33%)
6	13337	749.8	0.019	H-1(A)»L+1(A) (36%) HOMO(B)»L+1(B) (36%)	33	20107	497.3 0.001 H-4(A)»L+1(A) (10%) H-4(B)»L+1(B) (15%)
7	13501	740.7	0.005	HOMO(A)»L+1(A) (34%) HOMO(A)»L+4(A) (47%)	34	20189	495.3 0.002
8	14162	706.1	0.004	H-1(A)»LUMO(A) (21%) HOMO(A)»L+4(A) (22%) HOMO(B)»L+2(B) (22%)	35	20434	489.4 0.001 H-2(A)»L+1(A) (11%) H-2(B)»L+1(B) (11%)
9	14724	679.2	0.002	H-1(A)»L+2(A) (23%) H-1(A)»L+4(A) (12%) HOMO(A)»LUMO(A) (10%) HOMO(B)»L+3(B) (25%)	36	20672	483.7 0.002 H-1(A)»L+5(A) (13%)
10	14882	672.0	0.001	H-1(B)»LUMO(B) (64%)	37	20753	481.8 0.000 H-2(A)»L+4(A) (10%)
11	14908	670.8	0.017	HOMO(A)»L+5(A) (61%) HOMO(A)»L+6(A) (10%)	38	20954	477.2 0.002 H-5(B)»LUMO(B) (42%)
12	15131	660.9	0.028	H-2(B)»LUMO(B) (74%)	39	21112	473.7 0.003 H-3(A)»L+1(A) (18%) H-2(A)»LUMO(A) (24%) H-2(B)»L+2(B) (22%) H-1(B)»L+1(B) (16%)
13	15644	639.2	0.014	H-1(A)»L+3(A) (24%) H-1(B)»LUMO(B) (16%) HOMO(B)»L+4(B) (13%)	40	21154	472.7 0.001
14	16109	620.8	0.001	H-1(A)»L+2(A) (16%) H-1(A)»L+4(A) (25%) H-2(B)»LUMO(B) (12%) HOMO(B)»L+5(B) (18%)	41	21429	466.6 0.036 H-2(A)»L+2(A) (36%) H-2(B)»L+3(B) (23%) H-1(B)»L+2(B) (10%)
15	16651	600.6	0.001	H-3(B)»LUMO(B) (56%)	42	21531	464.4 0.086 HOMO(A)»L+8(A) (14%) H-2(B)»L+2(B) (18%) H-1(B)»L+1(B) (27%)
16	16876	592.6	0.093	H-1(A)»LUMO(A) (48%) HOMO(B)»L+2(B) (50%)	43	21634	462.2 0.155 H-3(A)»LUMO(A) (10%) H-2(A)»L+1(A) (22%) H-2(A)»L+2(A) (10%) H-2(B)»L+1(B) (23%) H-1(B)»L+2(B) (10%)
17	16896	591.9	0.119	H-1(A)»L+1(A) (47%) HOMO(B)»L+1(B) (49%)	44	21658	461.7 0.025 H-1(A)»L+6(A) (31%) HOMO(B)»L+7(B) (20%)
18	17113	584.4	0.048	HOMO(A)»L+5(A) (12%) HOMO(A)»L+6(A) (11%) H-4(B)»LUMO(B) (54%)	45	21740	460.0 0.088 H-3(A)»L+1(A) (25%) H-2(A)»LUMO(A) (16%) H-1(B)»L+5(B) (13%)
19	17261	579.3	0.264	H-1(A)»L+2(A) (38%) HOMO(B)»L+3(B) (53%)	46	21852	457.6 0.022 H-3(A)»LUMO(A) (15%) H-2(A)»L+1(A) (29%) H-1(B)»L+2(B) (27%)
20	17327	577.1	0.031	H-1(A)»L+3(A) (30%) H-1(A)»L+5(A) (13%) HOMO(B)»L+6(B) (13%)	47	21999	454.6 0.004 H-3(A)»LUMO(A) (19%) H-2(B)»L+1(B) (18%) HOMO(B)»L+8(B) (11%)
21	17652	566.5	0.025	HOMO(A)»L+6(A) (51%) HOMO(B)»L+5(B) (17%)	48	22017	454.2 0.020 H-3(A)»L+4(A) (13%) HOMO(A)»L+8(A) (15%) H-1(B)»L+5(B) (10%)
22	17805	561.6	0.470	H-1(A)»L+3(A) (21%) HOMO(B)»L+4(B) (51%)	49	22120	452.1 0.008 H-1(A)»L+7(A) (12%) H-6(B)»LUMO(B) (38%) HOMO(B)»L+8(B) (11%)
23	18047	554.1	0.347	H-1(A)»L+4(A) (37%) H-4(B)»LUMO(B) (11%) HOMO(B)»L+5(B) (35%)	50	22197	450.5 0.001 H-2(A)»L+3(A) (13%) H-4(B)»L+2(B) (14%) H-3(B)»L+1(B) (14%) H-1(B)»L+3(B) (18%)
24	18699	534.8	0.008	H-2(A)»LUMO(A) (10%) HOMO(A)»L+7(A) (33%)	51	22325	447.9 0.000 H-3(A)»L+2(A) (38%) H-2(B)»L+4(B) (11%)
25	19005	526.2	0.003	H-1(B)»L+2(B) (13%)	52	22348	447.5 0.007 H-1(B)»L+4(B) (49%)
26	19106	523.4	0.015	H-3(A)»L+1(A) (11%) HOMO(A)»L+7(A) (10%) H-1(B)»L+1(B) (14%)	53	22415	446.1 0.014 H-2(A)»L+3(A) (19%) H-2(B)»L+4(B) (28%) H-1(B)»L+3(B) (18%)
27	19305	518.0	0.016	HOMO(A)»L+7(A) (36%) H-8(B)»LUMO(B) (10%)	54	22450	445.4 0.059 H-3(A)»L+3(A) (56%) H-1(B)»L+4(B) (11%)
					55	22524	444.0 0.001 HOMO(B)»L+7(B) (14%)
					56	22546	443.5 0.002 HOMO(B)»L+8(B) (13%)

57	22692	440.7	0.017	H-1(A)»L+6(A) (35%) HOMO(A)»L+8(A) (11%) HOMO(B)»L+7(B) (22%)	82	24496	408.2	0.060	H-2(A)»L+7(A) (12%) H-2(B)»L+8(B) (11%) H-1(B)»L+6(B) (35%)
58	22755	439.5	0.002	H-2(A)»L+4(A) (33%) H-9(B)»LUMO(B) (12%)	83	24521	407.8	0.005	H-4(A)»L+3(A) (11%) H-16(B)»LUMO(B) (15%) H-4(B)»L+4(B) (23%)
59	22837	437.9	0.005	HOMO(A)»L+8(A) (18%)	84	24605	406.4	0.020	H-19(B)»LUMO(B) (16%)
60	22923	436.2	0.001	H-3(A)»L+2(A) (13%) H-7(B)»LUMO(B) (27%)	85	24693	405.0	0.016	H-3(A)»L+5(A) (12%) H-1(A)»L+8(A) (17%)
61	23121	432.5	0.003		86	24764	403.8	0.013	H-18(B)»LUMO(B) (20%)
62	23131	432.3	0.009	H-5(A)»LUMO(A) (13%) H-3(B)»L+2(B) (18%) H-2(B)»L+5(B) (15%)	87	24765	403.8	0.001	H-4(A)»L+3(A) (20%)
63	23159	431.8	0.000	H-5(A)»L+1(A) (12%) H-8(B)»LUMO(B) (28%) H-7(B)»LUMO(B) (27%)	88	24789	403.4	0.000	H-11(A)»L+1(A) (14%)
64	23221	430.7	0.067	H-5(A)»L+1(A) (20%) H-4(B)»L+2(B) (15%) H-3(B)»L+1(B) (12%)	89	24800	403.2	0.005	H-12(A)»L+1(A) (19%) H-14(B)»L+1(B) (18%)
65	23347	428.3	0.011	H-4(A)»LUMO(A) (42%) H-4(B)»L+2(B) (12%)	90	24839	402.6	0.011	H-16(B)»LUMO(B) (12%)
66	23354	428.2	0.150	H-5(A)»L+3(A) (14%) H-1(A)»L+7(A) (16%) H-2(B)»L+5(B) (12%) HOMO(B)»L+8(B) (11%)	91	24852	402.4	0.054	H-5(A)»LUMO(A) (14%) H-3(A)»L+5(A) (33%) H-1(B)»L+6(B) (17%)
67	23420	427.0	0.035	H-4(A)»L+2(A) (12%) H-1(A)»L+7(A) (17%) H-4(B)»L+3(B) (16%) HOMO(B)»L+8(B) (19%)	92	24995	400.1	0.005	H-5(A)»L+4(A) (11%) H-2(A)»L+5(A) (23%) H-2(B)»L+6(B) (21%)
68	23497	425.6	0.000	H-12(B)»LUMO(B) (55%)	93	25207	396.7	0.018	H-4(A)»L+1(A) (10%)
69	23499	425.6	0.000	H-15(B)»LUMO(B) (21%) H-10(B)»LUMO(B) (41%)	94	25229	396.4	0.020	H-16(B)»LUMO(B) (15%)
70	23591	423.9	0.081	H-9(A)»LUMO(B) (22%) H-3(B)»L+4(B) (16%)	95	25298	395.3	0.003	H-17(B)»LUMO(B) (10%)
71	23742	421.2	0.058	H-3(A)»L+4(A) (21%) H-4(B)»L+2(B) (12%) H-1(B)»L+5(B) (24%)	96	25482	392.4	0.002	H-4(A)»L+4(A) (16%)
72	23774	420.6	0.044	H-5(A)»LUMO(A) (10%) H-4(A)»L+1(A) (12%) H-4(B)»L+1(B) (33%) H-3(B)»L+2(B) (15%)	97	25486	392.4	0.089	H-5(A)»L+4(A) (23%) H-4(A)»L+3(A) (12%) H-2(A)»L+5(A) (10%) H-3(B)»L+5(B) (11%)
73	23851	419.3	0.054	H-4(A)»L+2(A) (14%) H-4(B)»L+3(B) (20%)	98	25519	391.9	0.037	H-17(B)»LUMO(B) (14%) H-4(B)»L+5(B) (38%)
74	23937	417.8	0.061	H-5(A)»L+1(A) (10%) H-3(A)»L+4(A) (10%) H-2(A)»L+5(A) (17%) H-2(B)»L+6(B) (18%)	99	25566	391.1	0.002	
75	23983	417.0	0.056	HOMO(A)»L+9(A) (64%)	100	25584	390.9	0.007	H-4(A)»L+4(A) (29%)
76	23988	416.9	0.014	H-5(A)»L+2(A) (20%) H-3(B)»L+3(B) (46%)	101	25595	390.7	0.105	H-5(A)»L+4(A) (19%)
77	24065	415.5	0.046	H-4(A)»L+1(A) (17%) H-4(A)»L+2(A) (15%)	102	25639	390.0	0.010	H-17(B)»LUMO(B) (15%)
78	24187	413.4	0.028	H-5(A)»L+2(A) (17%) H-2(B)»L+6(B) (10%)	103	25683	389.4	0.002	
79	24203	413.2	0.151	H-5(A)»L+3(A) (30%) H-3(B)»L+4(B) (35%)	104	25752	388.3	0.001	
80	24452	409.0	0.008	H-13(B)»LUMO(B) (16%) H-13(B)»L+3(B) (10%) H-11(B)»L+2(B) (11%)	105	26050	383.9	0.003	H-14(A)»LUMO(A) (18%) H-13(A)»L+2(A) (17%) H-11(B)»LUMO(B) (30%)
81	24464	408.8	0.001	H-13(B)»L+2(B) (15%) H-11(B)»LUMO(B) (20%) H-11(B)»L+3(B) (13%)	106	26053	383.8	0.000	H-14(A)»L+2(A) (17%) H-13(A)»LUMO(A) (23%) H-13(B)»LUMO(B) (37%)
					107	26130	382.7	0.007	H-26(B)»LUMO(B) (11%) H-20(B)»LUMO(B) (16%) H-3(B)»L+6(B) (23%)
					108	26241	381.1	0.000	
					109	26288	380.4	0.000	H-5(B)»L+2(B) (12%) H-1(B)»L+7(B) (14%)
					110	26377	379.1	0.001	H-15(A)»L+2(A) (21%) H-15(A)»L+3(A) (30%) H-15(A)»L+4(A) (11%)
					111	26378	379.1	0.000	H-16(A)»L+2(A) (21%) H-16(A)»L+3(A) (30%) H-16(A)»L+4(A) (11%)

112	26453	378.0	0.021	H-3(A)»L+6(A) (13%) H-5(B)»L+2(B) (13%)				HOMO(A)»L+14(A) (11%)
113	26490	377.5	0.002	H-12(A)»L+1(A) (14%) H-14(B)»LUMO(B) (53%)				H-8(A)»LUMO(A) (12%) H-7(B)»L+2(B) (17%)
114	26496	377.4	0.001	H-11(A)»L+1(A) (13%) H-15(B)»LUMO(B) (26%) H-10(B)»LUMO(B) (14%)				H-4(A)»L+5(A) (10%) H-7(B)»L+1(B) (13%)
115	26578	376.3	0.002	H-5(B)»L+1(B) (23%)				H-6(A)»LUMO(A) (16%) H-6(B)»L+2(B) (13%) H-2(B)»L+7(B) (12%)
116	26620	375.7	0.021	H-5(A)»L+5(A) (12%) H-1(A)»L+8(A) (15%)				H-7(A)»LUMO(A) (12%) H-7(A)»L+3(A) (14%)
117	26630	375.5	0.003	H-1(B)»L+7(B) (10%)				H-5(B)»L+3(B) (13%)
118	26655	375.2	0.002	H-3(A)»L+7(A) (13%) H-1(B)»L+8(B) (26%)				H-26(B)»LUMO(B) (17%) H-20(B)»LUMO(B) (21%)
119	26708	374.4	0.033	HOMO(B)»L+9(B) (42%)				H-21(B)»LUMO(B) (13%) H-19(B)»LUMO(B) (13%)
120	26776	373.5	0.010	H-11(A)»L+1(A) (11%) H-15(B)»LUMO(B) (19%) H-10(B)»LUMO(B) (11%)				H-6(A)»L+2(A) (12%) H-26(B)»LUMO(B) (11%) H-20(B)»LUMO(B) (12%) H-7(B)»L+2(B) (13%)
121	26791	373.3	0.001	H-12(A)»L+1(A) (14%) H-14(B)»LUMO(B) (34%) H-14(B)»L+1(B) (19%)				H-5(A)»L+5(A) (11%) H-5(B)»L+2(B) (21%)
122	26931	371.3	0.000					H-4(A)»L+5(A) (12%) H-22(B)»LUMO(B) (10%) H-4(B)»L+6(B) (18%)
123	26949	371.1	0.006					H-2(A)»L+6(A) (26%) H-5(B)»L+3(B) (10%)
124	27012	370.2	0.032					H-7(A)»LUMO(A) (37%) H-5(B)»L+2(B) (10%)
125	27039	369.8	0.012					H-2(B)»L+7(B) (16%)
126	27067	369.5	0.014					H-22(B)»LUMO(B) (22%) H-21(B)»LUMO(B) (13%)
127	27139	368.5	0.033					H-6(B)»L+1(B) (13%)
128	27222	367.3	0.003					HOMO(A)»L+10(A) (24%) H-11(B)»LUMO(B) (11%)
129	27248	367.0	0.009					H-13(B)»LUMO(B) (16%) H-13(B)»L+3(B) (10%) H-11(B)»L+2(B) (12%)
130	27260	366.8	0.004					HOMO(A)»L+10(A) (16%) H-13(B)»L+2(B) (10%) H-11(B)»LUMO(B) (12%)
131	27267	366.7	0.003					H-7(A)»L+1(A) (16%)
132	27342	365.7	0.004					H-4(A)»L+5(A) (10%) H-6(B)»L+2(B) (11%)
133	27429	364.6	0.006					H-6(A)»L+1(A) (17%) H-3(A)»L+6(A) (11%) H-6(B)»L+1(B) (24%)
134	27484	363.8	0.112					H-8(A)»L+1(A) (10%) H-7(B)»L+1(B) (10%) H-5(B)»L+3(B) (14%) HOMO(B)»L+10(B) (11%)
135	27499	363.6	0.189					HOMO(A)»L+11(A) (46%)
136	27537	363.2	0.018					137 27554 362.9 0.055 H-8(A)»LUMO(A) (12%) H-7(B)»L+2(B) (17%)
								138 27595 362.4 0.047 H-4(A)»L+5(A) (10%) H-7(B)»L+1(B) (13%)
								139 27673 361.4 0.017 H-6(A)»LUMO(A) (16%) H-6(B)»L+2(B) (13%) H-2(B)»L+7(B) (12%)
								140 27674 361.3 0.062 H-7(A)»LUMO(A) (12%) H-7(A)»L+3(A) (14%)
								141 27689 361.2 0.011 H-5(B)»L+3(B) (13%)
								142 27712 360.8 0.004 H-26(B)»LUMO(B) (17%) H-20(B)»LUMO(B) (21%)
								143 27758 360.3 0.003 H-21(B)»LUMO(B) (13%) H-19(B)»LUMO(B) (13%)
								144 27812 359.6 0.113 H-6(A)»L+2(A) (12%) H-26(B)»LUMO(B) (11%) H-20(B)»LUMO(B) (12%) H-7(B)»L+2(B) (13%)
								145 27878 358.7 0.013
								146 27879 358.7 0.016
								147 27947 357.8 0.052 HOMO(A)»L+12(A) (14%)
								148 27977 357.4 0.023 H-8(A)»LUMO(A) (12%)
								149 27988 357.3 0.001 H-31(B)»LUMO(B) (35%)
								150 27995 357.2 0.061 H-10(A)»LUMO(A) (11%) H-8(A)»L+2(A) (10%) H-7(B)»L+3(B) (15%)
								151 28014 357.0 0.007 H-32(B)»LUMO(B) (38%)
								152 28036 356.7 0.001
								153 28139 355.4 0.012 H-23(B)»LUMO(B) (13%) H-18(B)»LUMO(B) (18%)
								154 28154 355.2 0.037 H-5(B)»L+4(B) (12%)
								155 28166 355.0 0.014 H-7(A)»L+2(A) (15%)
								156 28219 354.4 0.003
								157 28254 353.9 0.051 H-6(A)»L+3(A) (24%) H-6(B)»L+4(B) (10%)
								158 28322 353.1 0.001 H-6(A)»LUMO(A) (11%) H-6(B)»L+4(B) (11%)
								159 28412 352.0 0.049
								160 28417 351.9 0.022 H-12(B)»LUMO(B) (11%) H-12(B)»L+3(B) (10%) H-10(B)»L+4(B) (13%)
								161 28425 351.8 0.009 H-12(B)»L+4(B) (23%) H-10(B)»LUMO(B) (10%) H-10(B)»L+3(B) (10%)
								162 28443 351.6 0.027
								163 28459 351.4 0.061 H-3(A)»L+7(A) (13%) H-1(A)»L+9(A) (26%) HOMO(B)»L+10(B) (23%)
								164 28488 351.0 0.006 H-8(B)»L+2(B) (14%)
								165 28516 350.7 0.006 H-10(A)»L+1(A) (15%) H-9(B)»L+1(B) (23%)

166	28577	349.9	0.001	H-24(B)»LUMO(B) (34%)		187	29202	342.4	0.029	HOMO(A)»L+13(A) (11%)
167	28630	349.3	0.012			188	29290	341.4	0.038	HOMO(A)»L+16(A) (13%)
168	28677	348.7	0.000			189	29305	341.2	0.007	H-7(B)»L+4(B) (20%)
169	28720	348.2	0.001	H-8(A)»L+2(A) (13%) H-24(B)»LUMO(B) (16%)		190	29378	340.4	0.002	H-3(B)»L+8(B) (11%)
170	28748	347.9	0.002			191	29379	340.4	0.021	HOMO(A)»L+13(A) (18%)
171	28779	347.5	0.006	H-8(A)»L+3(A) (17%) H-8(B)»L+2(B) (13%)		192	29392	340.2	0.044	HOMO(A)»L+16(A) (16%)
172	28810	347.1	0.003	H-8(B)»L+1(B) (66%)		193	29412	340.0	0.022	H-6(A)»L+4(A) (16%)
173	28833	346.8	0.003			194	29492	339.1	0.003	H-7(B)»L+4(B) (13%)
174	28838	346.8	0.002	H-34(B)»L+2(B) (12%) H-33(B)»LUMO(B) (12%) H-33(B)»L+3(B) (11%)		195	29536	338.6	0.060	H-5(B)»L+6(B) (12%)
175	28848	346.6	0.001			196	29661	337.1	0.052	H-8(A)»L+4(A) (31%)
176	28874	346.3	0.000	H-8(A)»L+2(A) (11%) H-9(B)»L+2(B) (16%) H-7(B)»L+3(B) (17%)		197	29662	337.1	0.025	H-6(B)»L+5(B) (22%)
177	28914	345.9	0.006	H-8(B)»L+2(B) (21%) H-3(B)»L+7(B) (13%)		198	29678	337.0	0.025	H-9(A)»LUMO(A) (33%)
178	28943	345.5	0.010	H-6(B)»L+4(B) (17%)		199	29713	336.5	0.057	H-6(B)»L+5(B) (10%)
179	28951	345.4	0.007	H-6(A)»L+4(A) (15%)		200	29797	335.6	0.054	H-9(A)»L+3(A) (14%)
180	28984	345.0	0.000	H-8(B)»L+3(B) (18%)					H-9(A)»L+3(A) (34%)	
181	29017	344.6	0.001						H-8(B)»L+4(B) (10%)	
182	29042	344.3	0.000	H-25(B)»LUMO(B) (48%) H-23(B)»LUMO(B) (16%)						
183	29060	344.1	0.001	H-31(A)»L+1(A) (12%) H-36(B)»L+1(B) (15%) H-25(B)»LUMO(B) (14%)						
184	29101	343.6	0.008	HOMO(A)»L+15(A) (10%)						
185	29140	343.2	0.001	H-8(A)»L+3(A) (10%) H-3(B)»L+7(B) (20%)						
186	29182	342.7	0.048	H-7(A)»L+4(A) (17%) H-8(B)»L+3(B) (16%) H-5(B)»L+5(B) (12%)						

[a] Oscillator strength. [b] Contributions smaller than 10% are not included. H = HOMO, L = LUMO. Orbitals are numbered consecutively regardless of possible degeneracies.

Table S4. Electronic transitions calculated for **4₂** using the TDA/B3LYP/3-21G level of theory.

No.	Energy (cm ⁻¹)	λ (nm)	f ^[a]	Major excitations ^[b]				
1	14807	675.4	0.001	HOMO»LUMO (73%)	27	19805	504.9	0.033
2	15087	662.8	0.005	H-1»LUMO (21%) HOMO»L+1 (65%)	28	19874	503.2	0.041
3	15595	641.2	0.010	HOMO»L+2 (76%)	29	20022	499.5	0.011
4	16209	617.0	0.010	H-1»L+1 (12%) H-1»L+2 (22%) HOMO»L+3 (49%)	30	20064	498.4	0.121
5	16308	613.2	0.021	H-1»LUMO (62%) HOMO»L+1 (21%)	31	20096	497.6	0.090
6	16567	603.6	0.017	H-1»L+1 (57%) H-1»L+2 (15%)	32	20304	492.5	0.009
7	16886	592.2	0.061	H-1»L+2 (45%) HOMO»L+3 (21%) HOMO»L+5 (11%)	33	20386	490.5	0.011
8	17030	587.2	0.145	HOMO»L+3 (10%) HOMO»L+4 (68%)	34	20530	487.1	0.022
9	17250	579.7	0.185	HOMO»L+5 (62%) HOMO»L+6 (11%)	35	20653	484.2	0.072
10	17431	573.7	0.075	H-1»L+3 (44%) HOMO»L+6 (36%)	36	20708	482.9	0.052
11	17571	569.1	0.074	H-1»L+3 (34%) HOMO»L+5 (17%) HOMO»L+6 (28%)	37	20741	482.1	0.055
12	17712	564.6	0.158	H-1»L+4 (56%) HOMO»L+6 (10%) HOMO»L+7 (19%)	38	20847	479.7	0.020
13	17960	556.8	0.107	H-2»LUMO (16%) H-1»L+5 (34%) HOMO»L+7 (16%)	39	20905	478.4	0.012
14	18075	553.3	0.016	H-2»LUMO (16%) H-1»L+4 (19%) HOMO»L+7 (40%)	40	20968	476.9	0.033
15	18205	549.3	0.019	H-2»LUMO (34%) H-2»L+1 (13%) HOMO»L+8 (22%)	41	21021	475.7	0.079
16	18344	545.1	0.061	H-1»L+5 (43%) HOMO»L+9 (19%)	42	21113	473.6	0.029
17	18415	543.0	0.200	H-1»L+5 (10%) H-1»L+6 (20%) HOMO»L+9 (44%)	43	21322	469.0	0.021
18	18476	541.3	0.201	H-2»L+1 (27%) HOMO»L+8 (50%)	44	21379	467.7	0.026
19	18578	538.3	0.105	H-2»L+1 (29%) H-1»L+6 (40%) HOMO»L+9 (12%)	45	21450	466.2	0.099
20	18929	528.3	0.047	H-1»L+7 (80%)	46	21545	464.1	0.008
21	19000	526.3	0.020	H-2»L+2 (71%)	47	21587	463.2	0.029
22	19265	519.1	0.099	H-3»LUMO (47%) H-1»L+9 (15%)	48	21700	460.8	0.014
23	19319	517.6	0.064	H-3»LUMO (15%) H-1»L+9 (51%)	49	21793	458.9	0.031
24	19457	514.0	0.100	H-1»L+8 (55%)	50	21875	457.1	0.009
25	19663	508.6	0.022	H-3»L+1 (31%) H-2»L+3 (17%) H-2»L+4 (10%) H-1»L+8 (10%)	51	21965	455.3	0.003
26	19679	508.2	0.046	H-3»L+1 (28%) H-2»L+4 (12%) H-1»L+9 (10%) HOMO»L+10 (24%)				

52	21991	454.7	0.014	H-6»L+1 (12%) H-2»L+9 (11%) H-1»L+12 (38%)	80	23446	426.5	0.013	H-8»L+2 (10%) H-5»L+5 (11%) H-1»L+13 (23%)
53	22128	451.9	0.003	H-4»L+4 (14%) H-3»L+7 (47%)	81	23519	425.2	0.020	H-9»L+2 (12%) H-7»L+2 (13%) H-5»L+6 (16%)
54	22141	451.7	0.040	H-6»L+2 (17%) H-5»L+2 (25%)	82	23581	424.1	0.002	H-8»L+2 (26%) H-1»L+13 (14%) HOMO»L+15 (21%)
55	22188	450.7	0.015	H-6»L+1 (35%) H-4»L+4 (13%)	83	23650	422.8	0.031	H-6»L+4 (17%) H-4»L+9 (12%)
56	22321	448.0	0.031	H-4»L+5 (54%)	84	23686	422.2	0.004	H-9»L+2 (27%) H-1»L+14 (22%)
57	22387	446.7	0.004	H-7»LUMO (10%) HOMO»L+13 (51%)	85	23774	420.6	0.005	H-3»L+10 (56%)
58	22406	446.3	0.075	H-4»L+6 (30%)	86	23830	419.6	0.092	H-9»L+2 (15%) H-2»L+12 (12%) H-1»L+14 (23%)
59	22469	445.1	0.019	H-6»L+2 (20%) H-5»L+2 (11%) H-4»L+7 (16%)	87	23881	418.7	0.015	H-6»L+5 (38%)
60	22496	444.5	0.027	H-9»LUMO (11%) H-7»LUMO (26%) HOMO»L+13 (15%)	88	23940	417.7	0.011	H-8»L+3 (22%) H-2»L+12 (20%)
61	22593	442.6	0.023	H-6»L+2 (17%) H-4»L+6 (14%) H-4»L+7 (11%)	89	23988	416.9	0.060	H-8»L+3 (11%) H-3»L+11 (17%) H-2»L+12 (11%)
62	22615	442.2	0.019	H-7»L+1 (12%) H-3»L+8 (27%) H-3»L+9 (17%)	90	24108	414.8	0.022	H-7»L+3 (13%) H-3»L+11 (35%)
63	22696	440.6	0.015	H-8»LUMO (14%) HOMO»L+14 (37%)	91	24131	414.4	0.012	H-9»L+3 (37%)
64	22748	439.6	0.022	H-2»L+10 (67%)	92	24208	413.1	0.002	H-6»L+6 (10%) H-5»L+7 (35%)
65	22781	439.0	0.016	H-3»L+9 (19%)	93	24235	412.6	0.048	H-9»L+3 (12%) H-7»L+3 (28%) H-3»L+11 (18%)
66	22838	437.9	0.025	H-8»LUMO (19%) H-3»L+8 (19%)	94	24328	411.0	0.028	H-8»L+4 (12%) H-7»L+4 (10%) H-6»L+7 (17%) HOMO»L+16 (10%)
67	22888	436.9	0.002	H-9»LUMO (14%) H-3»L+8 (14%) H-2»L+11 (25%)	95	24335	410.9	0.030	HOMO»L+16 (37%)
68	22913	436.4	0.020	H-2»L+11 (28%)	96	24381	410.1	0.032	H-8»L+4 (10%) H-7»L+4 (59%)
69	22934	436.0	0.047	H-6»L+3 (19%) H-5»L+3 (31%) H-2»L+11 (16%)	97	24469	408.7	0.006	H-6»L+5 (12%) H-6»L+6 (33%) H-5»L+5 (11%)
70	22979	435.2	0.019	H-8»LUMO (12%) H-7»L+1 (27%)	98	24575	406.9	0.001	H-27»LUMO (14%) H-27»L+1 (24%) H-27»L+3 (22%)
71	23038	434.1	0.013	H-8»L+1 (18%) H-6»L+3 (11%) H-5»L+4 (15%)	99	24582	406.8	0.009	H-2»L+12 (21%) H-1»L+15 (48%)
72	23117	432.6	0.051	H-6»L+3 (11%) H-5»L+3 (18%)	100	24612	406.3	0.002	H-7»L+5 (17%)
73	23196	431.1	0.043	H-6»L+4 (15%) H-4»L+9 (19%)	101	24624	406.1	0.003	H-5»L+8 (30%)
74	23217	430.7	0.013	H-9»L+1 (16%) H-9»L+2 (14%) H-8»L+1 (10%) H-4»L+8 (11%)	102	24656	405.6	0.026	H-8»L+5 (11%) H-7»L+5 (18%)
75	23268	429.8	0.014	H-9»L+1 (25%) H-8»L+1 (12%) H-7»L+2 (10%)	103	24684	405.1	0.002	H-24»L+2 (10%) H-7»L+5 (14%) H-5»L+8 (12%)
76	23317	428.9	0.005	H-7»L+2 (20%) H-5»L+4 (20%)	104	24761	403.9	0.009	H-8»L+4 (11%) H-7»L+5 (10%) H-6»L+8 (13%)
77	23339	428.5	0.037	H-8»L+2 (17%) H-5»L+5 (13%)	105	24801	403.2	0.005	H-21»L+4 (11%) H-21»L+5 (18%) H-21»L+6 (13%)
78	23384	427.6	0.007	H-8»L+2 (16%) HOMO»L+15 (27%)	106	24818	402.9	0.001	H-6»L+7 (11%)
79	23398	427.4	0.035	H-8»L+1 (26%) H-7»L+2 (25%) H-5»L+4 (10%)	107	24859	402.3	0.012	H-4»L+10 (22%) HOMO»L+17 (22%)

108	24918	401.3	0.006	H-6»L+8 (11%)		134	25803	387.5	0.020	H-2»L+14 (10%)
109	24931	401.1	0.000	H-18»L+5 (22%)						H-1»L+17 (10%)
				H-18»L+6 (33%)		135	25836	387.1	0.005	
110	24953	400.8	0.003	H-6»L+8 (12%)		136	25869	386.6	0.004	H-9»L+7 (53%)
111	24983	400.3	0.023	H-11»LUMO (11%)		137	25891	386.2	0.014	H-11»L+2 (29%)
				H-8»L+5 (14%)					H-10»L+2 (10%)	
				H-7»L+6 (13%)		138	25960	385.2	0.012	H-9»L+8 (10%)
112	24999	400.0	0.002	H-23»L+4 (14%)						H-7»L+8 (13%)
				H-23»L+7 (15%)		139	26048	383.9	0.004	H-2»L+14 (26%)
113	25022	399.7	0.003	H-6»L+9 (12%)		140	26087	383.3	0.007	H-1»L+17 (53%)
				HOMO»L+17 (10%)		141	26107	383.0	0.013	H-14»LUMO (11%)
114	25040	399.4	0.053	H-9»L+4 (14%)		142	26143	382.5	0.005	H-8»L+9 (19%)
				H-4»L+10 (19%)		143	26184	381.9	0.000	H-7»L+9 (16%)
115	25057	399.1	0.008	H-26»L+4 (20%)		144	26189	381.8	0.026	H-33»LUMO (12%)
				H-23»L+7 (15%)		145	26223	381.3	0.011	H-37»LUMO (10%)
116	25098	398.4	0.002	H-10»LUMO (18%)		146	26240	381.1	0.069	H-37»L+1 (13%)
				H-8»L+5 (11%)		147	26277	380.6	0.007	H-17»LUMO (14%)
117	25105	398.3	0.000	H-19»L+3 (10%)		148	26299	380.2	0.069	H-11»L+2 (10%)
				H-19»L+7 (14%)		149	26335	379.7	0.057	H-5»L+11 (20%)
				H-19»L+9 (20%)		150	26362	379.3	0.010	H-5»L+11 (12%)
118	25150	397.6	0.012	H-5»L+9 (10%)		151	26417	378.5	0.061	H-5»L+10 (14%)
119	25165	397.4	0.001	H-15»L+7 (16%)		152	26426	378.4	0.011	H-4»L+11 (11%)
				H-15»L+8 (23%)		153	26465	377.9	0.035	H-12»L+2 (14%)
120	25185	397.1	0.032	H-7»L+7 (14%)		154	26478	377.7	0.019	H-5»L+10 (12%)
				H-6»L+9 (19%)		155	26539	376.8	0.027	H-4»L+12 (10%)
				H-4»L+10 (13%)		156	26583	376.2	0.020	H-2»L+15 (18%)
121	25217	396.6	0.008	H-4»L+11 (35%)		157	26609	375.8	0.015	H-3»L+13 (10%)
				H-3»L+12 (11%)		158	26636	375.4	0.014	H-13»L+2 (12%)
122	25248	396.1	0.040	H-8»L+6 (28%)		159	26679	374.8	0.014	H-5»L+11 (11%)
				H-7»L+6 (13%)		160	26715	374.3	0.029	H-11»L+8 (10%)
123	25286	395.5	0.026	H-7»L+7 (23%)		161	26741	374.0	0.012	H-4»L+12 (17%)
124	25310	395.1	0.036	H-11»LUMO (29%)		162	26817	372.9	0.045	H-3»L+13 (13%)
				H-8»L+6 (10%)		163	26838	372.6	0.001	H-6»L+11 (11%)
				H-7»L+7 (19%)		164	26883	372.0	0.008	H-14»L+2 (19%)
125	25385	393.9	0.025	H-9»L+5 (12%)		165	26934	371.3	0.031	H-3»L+14 (19%)
				H-9»L+6 (10%)		166	26966	370.8	0.022	H-16»L+2 (19%)
				H-3»L+12 (19%)		167	27005	370.3	0.039	H-3»L+14 (10%)
126	25425	393.3	0.010	H-9»L+6 (13%)		168	27040	369.8	0.033	H-11»L+5 (28%)
				H-3»L+12 (28%)		169	27079	369.3	0.009	H-10»L+2 (12%)
127	25456	392.8	0.007	H-3»L+12 (12%)		170	27103	369.0	0.002	H-10»L+5 (11%)
				H-2»L+13 (26%)		171	27124	368.7	0.001	H-13»L+2 (14%)
				H-1»L+16 (23%)					H-16»LUMO (20%)	
128	25504	392.1	0.025	H-13»LUMO (12%)						H-15»LUMO (13%)
				H-11»L+1 (13%)						
129	25590	390.8	0.008	H-11»L+1 (18%)						
				H-10»LUMO (10%)						
				H-10»L+1 (20%)						
130	25621	390.3	0.005	H-8»L+7 (12%)						
				H-2»L+13 (23%)						
				H-2»L+14 (16%)						
				H-1»L+16 (18%)						
131	25658	389.7	0.021	H-8»L+7 (29%)						
				H-7»L+9 (11%)						
132	25704	389.0	0.005	H-8»L+7 (26%)						
				H-7»L+8 (11%)						
				H-7»L+9 (11%)						
133	25748	388.4	0.023	H-13»LUMO (10%)						
				H-12»LUMO (10%)						
				H-10»L+1 (10%)						
				H-10»L+2 (13%)						

				(34%)
				H-15»L+1 (17%)
172	27133	368.6	0.009	H-25»LUMO (11%)
173	27161	368.2	0.016	H-22»LUMO (14%) H-17»LUMO (17%)
174	27186	367.8	0.002	H-12»L+4 (11%)
175	27225	367.3	0.015	
176	27248	367.0	0.012	
177	27266	366.8	0.001	H-18»LUMO (49%) H-18»L+1 (33%)
178	27287	366.5	0.003	H-20»LUMO (28%) H-20»L+2 (15%)
179	27300	366.3	0.022	H-19»LUMO (13%)
180	27312	366.1	0.007	H-20»LUMO (12%) H-19»LUMO (40%) H-19»L+1 (13%)
181	27346	365.7	0.008	H-21»LUMO (39%) H-21»L+1 (13%)
182	27365	365.4	0.010	H-21»LUMO (12%)
183	27390	365.1	0.017	H-10»L+5 (10%)

184	27408	364.9	0.038	
185	27464	364.1	0.036	H-7»L+11 (15%)
186	27475	364.0	0.023	H-25»LUMO (12%)
187	27503	363.6	0.010	H-7»L+10 (11%) H-5»L+12 (10%) H-4»L+14 (10%)
188	27510	363.5	0.005	H-11»L+5 (12%)
189	27561	362.8	0.027	H-12»L+3 (12%) H-8»L+10 (10%)
190	27594	362.4	0.011	H-8»L+10 (30%)
191	27618	362.1	0.016	H-11»L+6 (28%)
192	27629	361.9	0.050	H-25»L+1 (11%)
193	27648	361.7	0.016	H-11»L+7 (16%)
194	27667	361.4	0.019	H-11»L+7 (10%) H-10»L+7 (11%)
195	27685	361.2	0.023	H-12»L+3 (10%)
196	27714	360.8	0.020	H-14»L+4 (15%)
197	27734	360.6	0.022	H-7»L+11 (11%)
198	27772	360.1	0.037	H-8»L+11 (13%)
199	27787	359.9	0.017	H-5»L+12 (11%)
200	27806	359.6	0.011	H-20»L+1 (10%)

[a] Oscillator strength. [b] Contributions smaller than 10% are not included. H = HOMO, L = LUMO. Orbitals are numbered consecutively regardless of possible degeneracies.

Table S5. Electronic transitions calculated for **7** using the TDA/B3LYP/6-31G(d,p) level of theory.

No.	Energy (cm ⁻¹)	λ (nm)	f ^[a]	Major excitations ^[b]				
1	15851	630.9	0.149	HOMO»LUMO (93%)	32	24761	403.9	0.017
2	16946	590.1	0.110	HOMO»L+1 (99%)	33	25181	397.1	0.035
3	16983	588.8	0.139	HOMO»L+2 (98%)	34	25495	392.2	0.527
4	17447	573.2	0.330	HOMO»L+3 (95%)	35	25796	387.7	0.055
5	18072	553.4	0.409	HOMO»L+4 (96%)	36	25902	386.1	0.020
6	18364	544.5	0.072	HOMO»L+5 (88%)	37	25903	386.1	0.077
7	19986	500.4	0.053	H-1»LUMO (87%)	38	26253	380.9	0.063
8	20249	493.8	0.001	H-1»L+2 (12%) HOMO»L+6 (72%)	39	26278	380.6	0.003
9	20500	487.8	0.242	H-1»L+1 (96%)	40	26368	379.2	0.193
10	20545	486.7	0.059	H-1»L+2 (79%) HOMO»L+6 (10%)	41	26442	378.2	0.000
11	20583	485.8	0.013	H-2»LUMO (91%)	42	26475	377.7	0.010
12	21159	472.6	0.011	H-2»L+1 (11%) H-1»L+3 (74%)	43	26517	377.1	0.039
13	21391	467.5	0.008	H-1»L+4 (83%)	44	26559	376.5	0.033
14	21470	465.8	0.081	H-3»LUMO (18%) H-2»L+1 (56%)	45	26579	376.2	0.006
15	21827	458.1	0.125	H-3»LUMO (53%)	46	26608	375.8	0.017
16	21863	457.4	0.008	H-2»L+2 (44%) H-2»L+3 (21%) H-1»L+4 (11%)	47	26661	375.1	0.021
17	21957	455.4	0.031	H-2»L+2 (20%) H-2»L+3 (61%)	48	26748	373.9	0.103
18	22148	451.5	0.006	H-3»L+2 (75%)	49	26777	373.5	0.008
19	22430	445.8	0.142	H-4»LUMO (67%) H-2»L+2 (10%)	50	26952	371.0	0.002
20	22482	444.8	0.008	HOMO»L+7 (76%)				
21	22674	441.0	0.010	H-3»L+1 (57%) H-2»L+2 (11%)				
22	22867	437.3	0.023	H-1»L+5 (61%) HOMO»L+7 (13%)				
23	23154	431.9	0.094	H-4»L+1 (61%) H-3»L+3 (20%)				
24	23237	430.4	0.005	HOMO»L+8 (80%)				
25	23422	427.0	0.016	H-2»L+4 (51%) H-1»L+5 (11%)				
26	23581	424.1	0.033	H-4»L+2 (14%) H-4»L+3 (15%) H-3»L+4 (10%) H-1»L+6 (37%)				
27	23657	422.7	0.024	H-4»L+1 (13%) H-3»L+3 (64%) H-2»L+4 (14%)				
28	23693	422.1	0.093	H-4»L+2 (26%) H-3»L+1 (11%) H-3»L+4 (13%) H-1»L+6 (26%)				
29	23757	420.9	0.111	H-4»L+2 (33%) H-3»L+4 (34%) H-2»L+5 (13%)				
30	23930	417.9	0.129	H-4»L+3 (52%) H-1»L+6 (21%)				
31	24307	411.4	0.290	H-3»L+4 (18%) H-2»L+5 (68%)				

[a] Oscillator strength. [b] Contributions smaller than 10% are not included. H = HOMO, L = LUMO. Orbitals are numbered consecutively regardless of possible degeneracies.

NMR Spectra

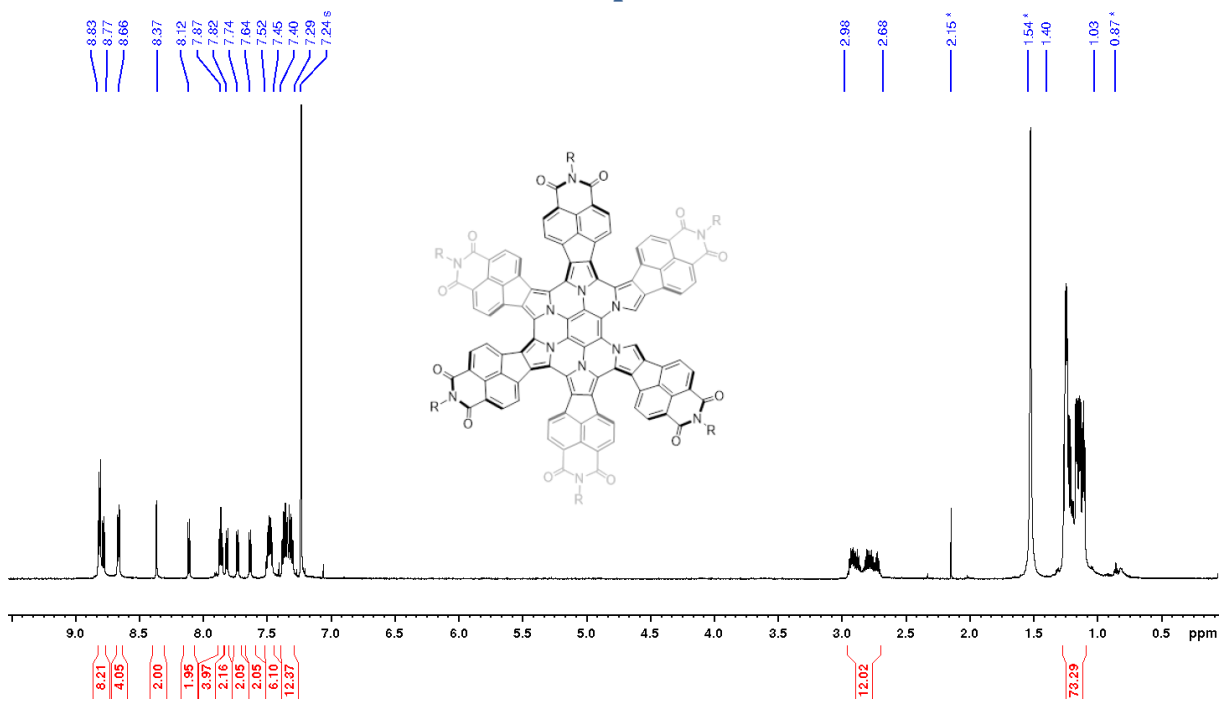


Figure S28. ¹H NMR spectrum of 6 (600 MHz, chloroform-d , 300 K).

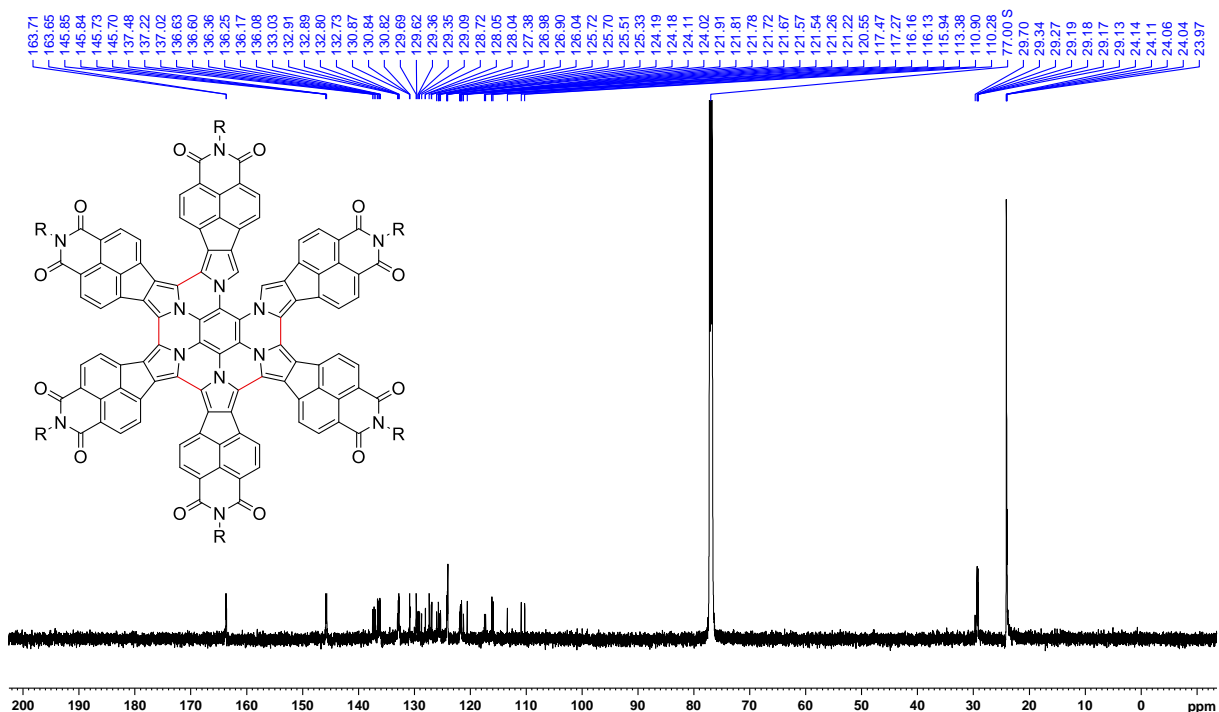


Figure S29. ¹³C NMR spectrum of 6 (151 MHz, chloroform-d, 300 K).

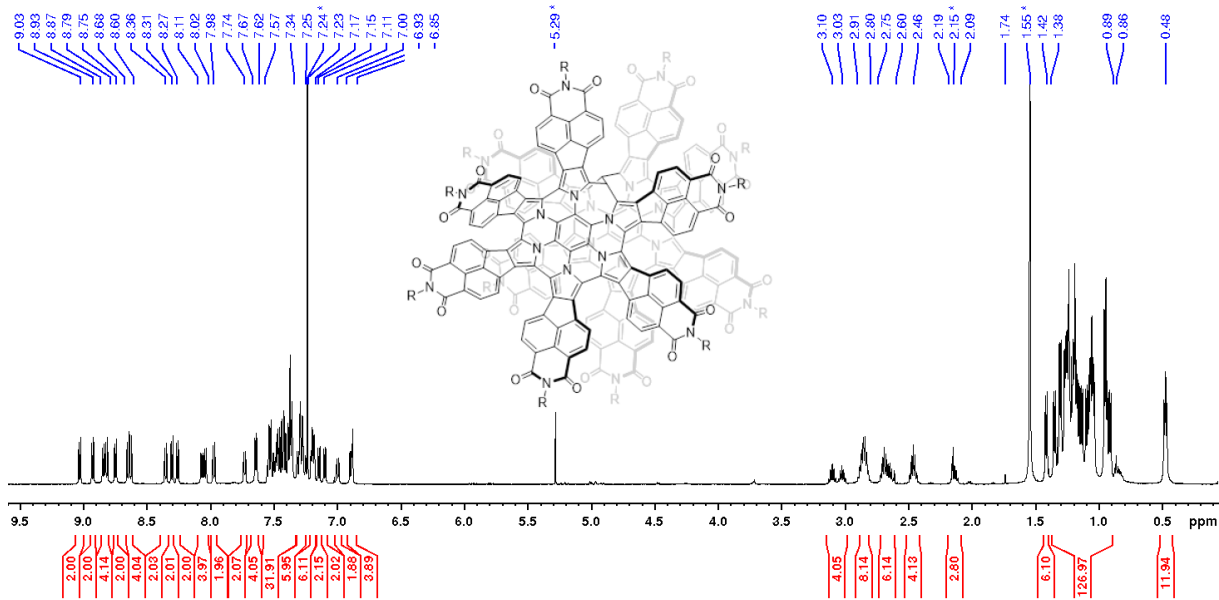


Figure S30. ^1H NMR spectrum of **4₂** (600 MHz, chloroform-*d*, 300 K).

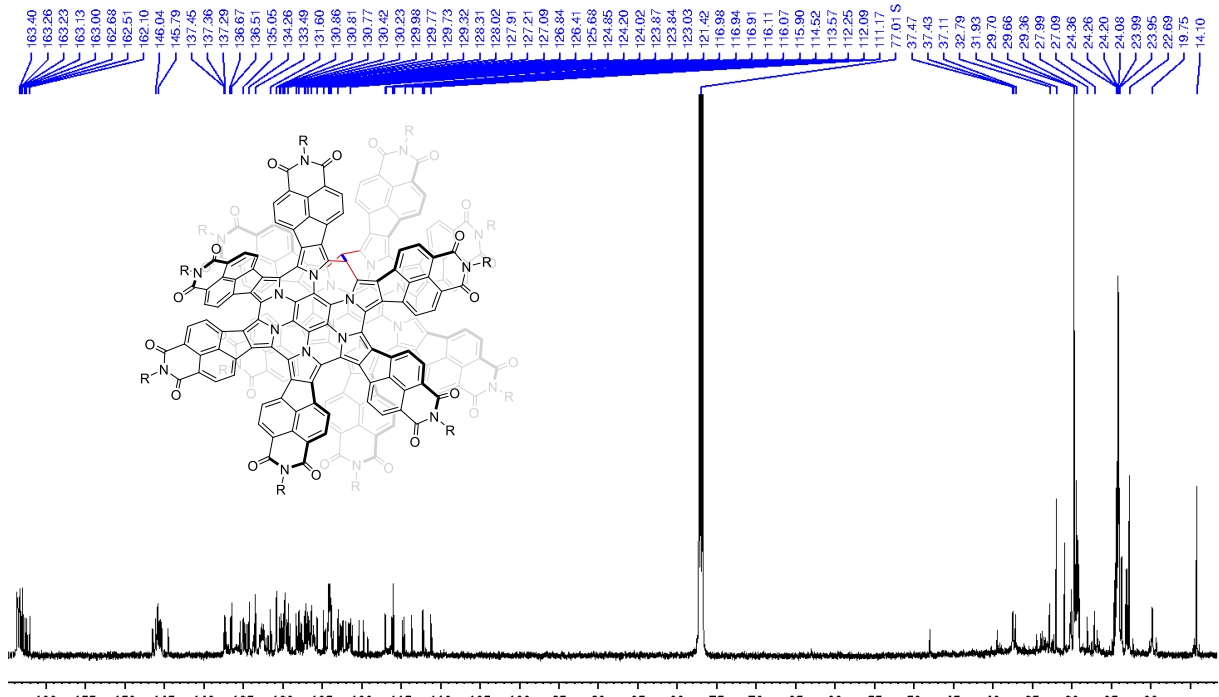


Figure S31. ^{13}C NMR spectrum of **4₂** (151 MHz, chloroform-*d*, 300 K).

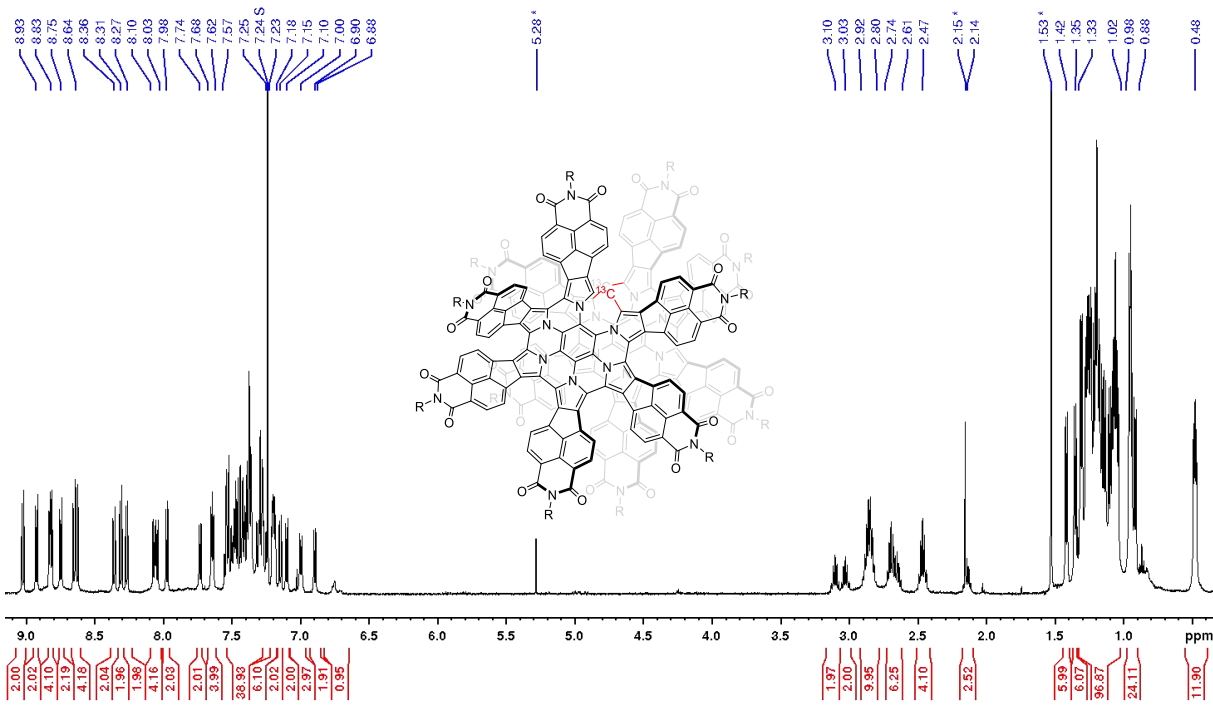


Figure S32. ¹H NMR spectrum of **4₂-C₂** (600 MHz, chloroform-d, 300 K).

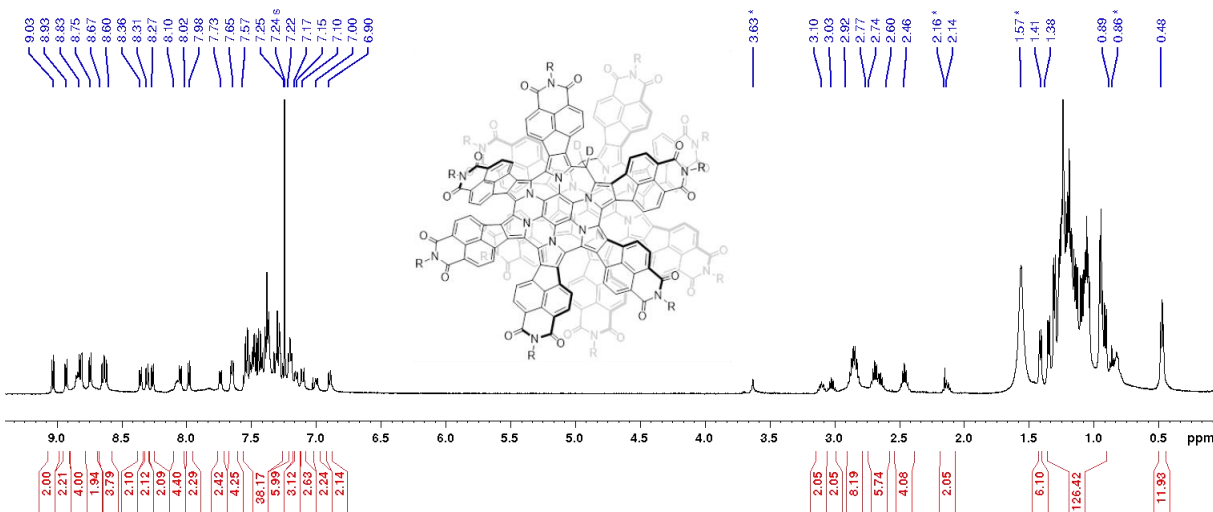


Figure S33. ¹H NMR spectrum of **4₂-d₂** (600 MHz, chloroform-d, 300 K).

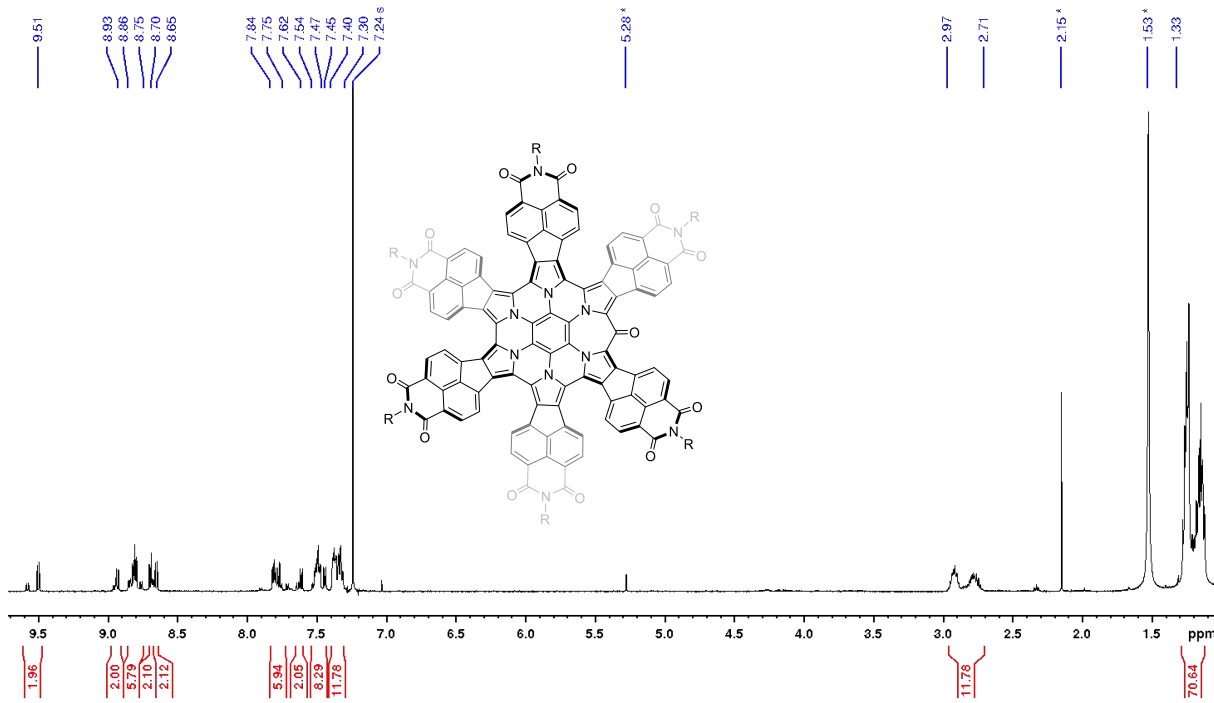


Figure S34. ^1H NMR spectrum of **7** (600 MHz, chloroform-*d*, 300 K).

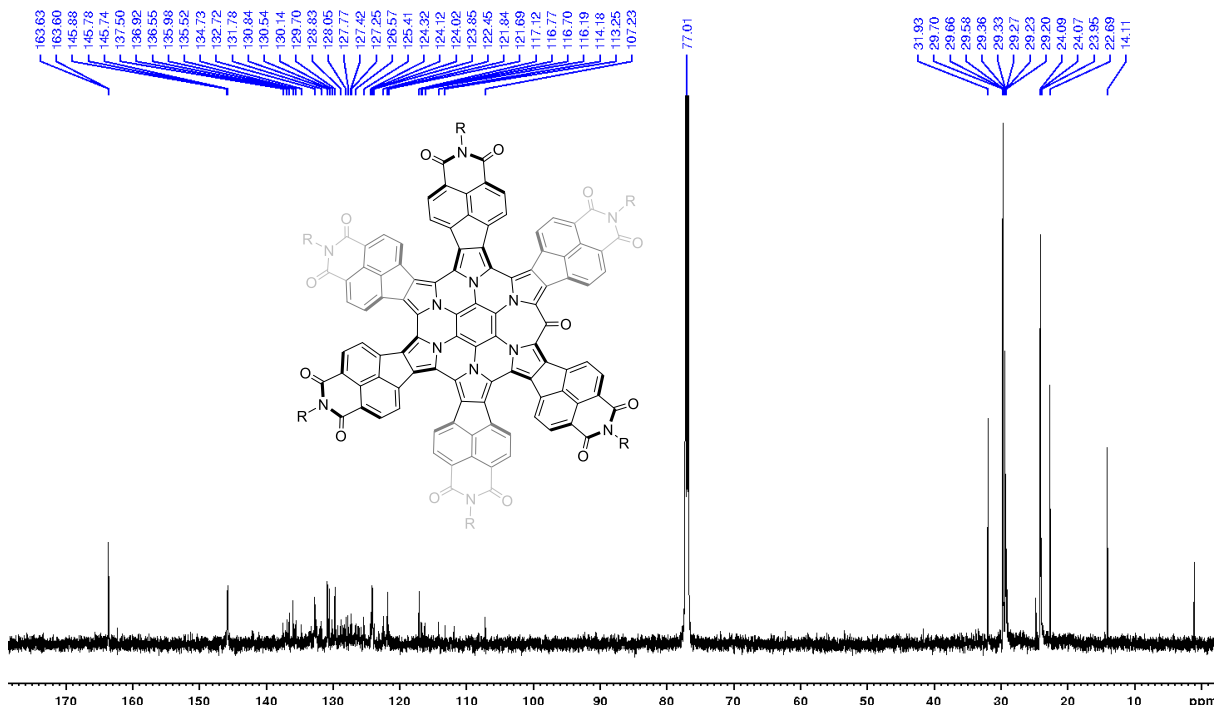


Figure S35. ^{13}C NMR spectrum of **7** (151 MHz, chloroform-*d*, 300 K).

Mass Spectra

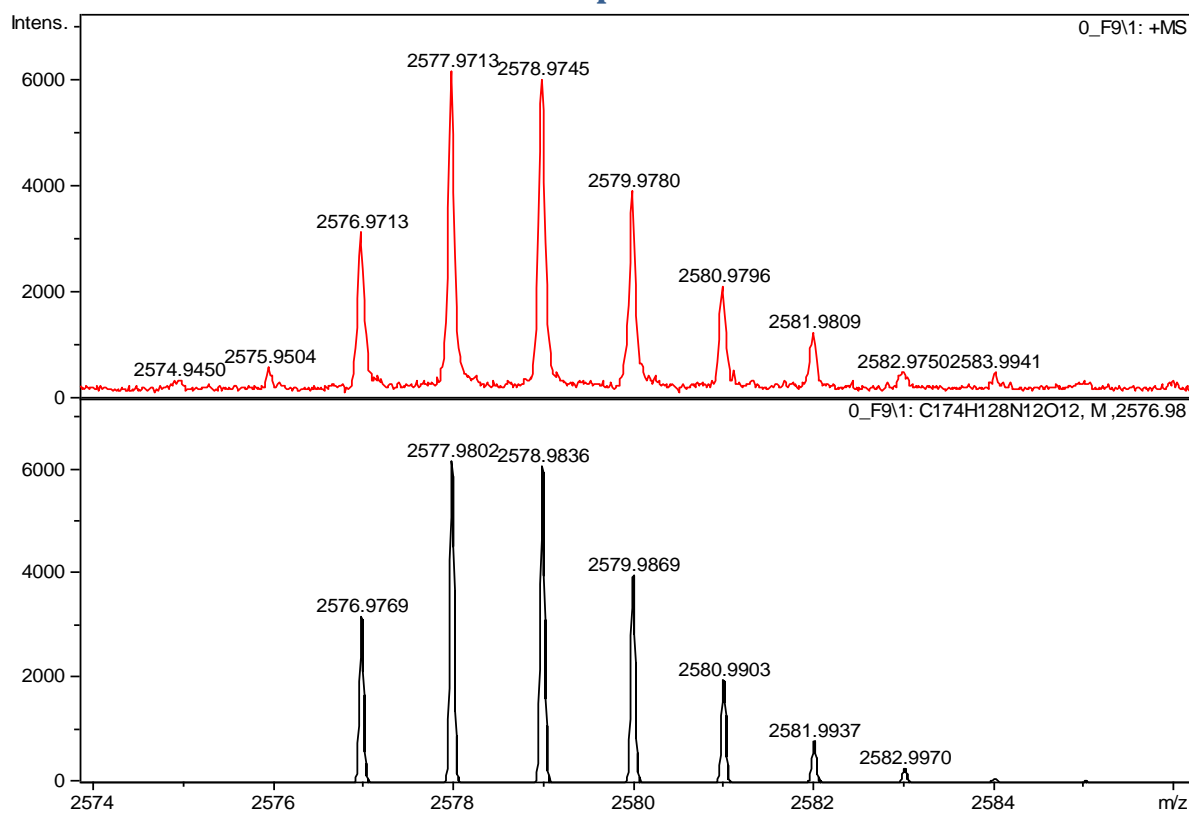


Figure S36. High resolution mass spectrum of **6** (MALDI–TOF, top: experimental, bottom: simulated).

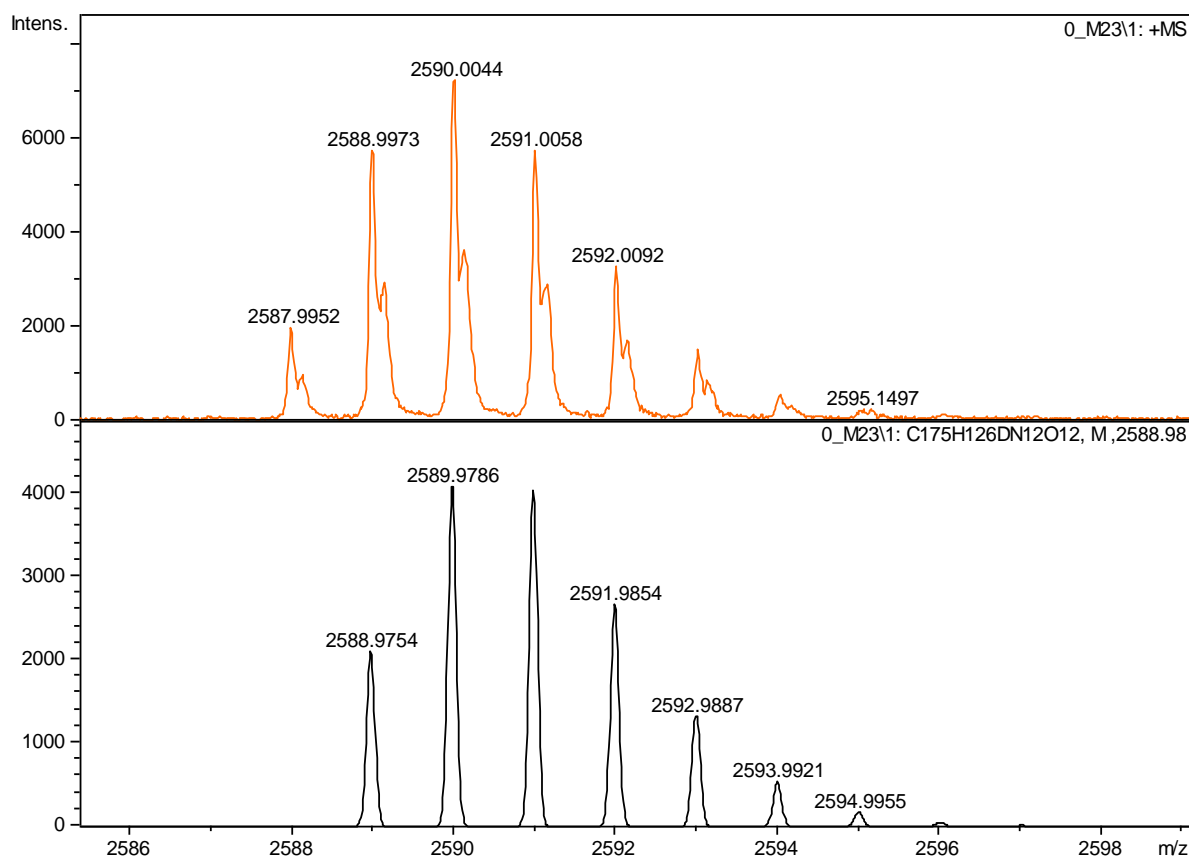


Figure S37. High resolution mass spectrum of **4-d** (MALDI–TOF, top: experimental, bottom: simulated).

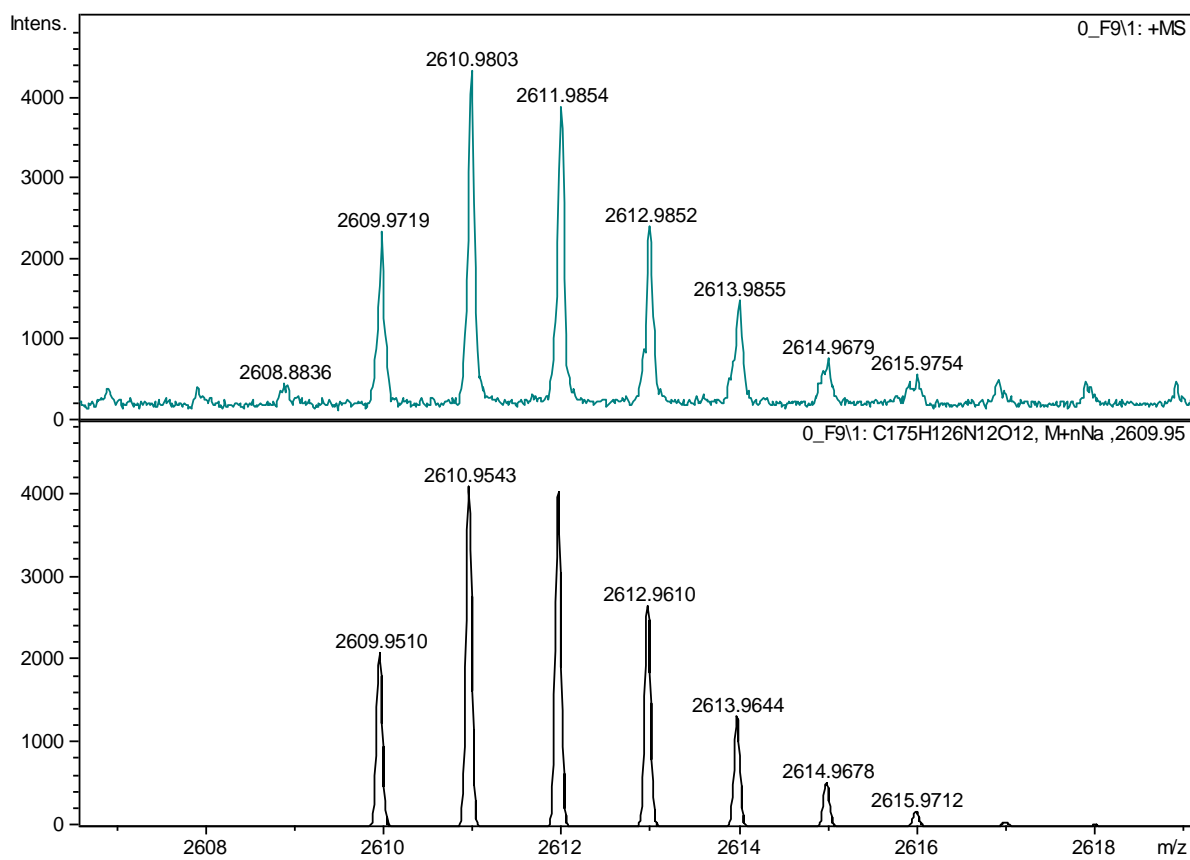


Figure S38. High resolution mass spectrum of **7** (MALDI-TOF, top: experimental, bottom: simulated).

References

- (1) Żyła-Karwowska, M.; Zhylitskaya, H.; Cybińska, J.; Lis, T.; Chmielewski, P. J.; Stępień, M. An Electron-Deficient Azacoronene Obtained by Radial π Extension. *Angew. Chem. Int. Ed.* **2016**, *55* (47), 14658–14662. <https://doi.org/10.1002/anie.201608400>.
- (2) Frisch, M. J.; Trucks, G. W.; Schlegel, H. B.; Scuseria, G. E.; Robb, M. A.; Cheeseman, J. R.; Scalmani, G.; Barone, V.; Petersson, G. A.; Nakatsuji, H.; Li, X.; Caricato, M.; Marenich, A. V.; Bloino, J.; Janesko, B. G.; Gomperts, R.; Mennucci, B.; Hratchian, H. P.; Ortiz, J. V.; Izmaylov, A. F.; Sonnenberg, J. L.; Williams-Young, D.; Ding, F.; Lipparini, F.; Egidi, F.; Goings, J.; Peng, B.; Petrone, A.; Henderson, T.; Ranasinghe, D.; Zakrzewski, V. G.; Gao, J.; Rega, N.; Zheng, G.; Liang, W.; Hada, M.; Ehara, M.; Toyota, K.; Fukuda, R.; Hasegawa, J.; Ishida, M.; Nakajima, T.; Honda, Y.; Kitao, O.; Nakai, H.; Vreven, T.; Throssell, K.; Montgomery, J. A., Jr.; Peralta, J. E.; Ogliaro, F.; Bearpark, M. J.; Heyd, J. J.; Brothers, E. N.; Kudin, K. N.; Staroverov, V. N.; Keith, T. A.; Kobayashi, R.; Normand, J.; Raghavachari, K.; Rendell, A. P.; Burant, J. C.; Iyengar, S. S.; Tomasi, J.; Cossi, M.; Millam, J. M.; Klene, M.; Adamo, C.; Cammi, R.; Ochterski, J. W.; Martin, R. L.; Morokuma, K.; Farkas, O.; Foresman, J. B.; Fox, D. J. *Gaussian 16, Revision B.01*; Wallingford CT, 2016.
- (3) Becke, A. D. Density-Functional Exchange-Energy Approximation with Correct Asymptotic Behavior. *Phys. Rev. A* **1988**, *38* (6), 3098–3100.
- (4) Becke, A. D. Density-functional Thermochemistry. III. The Role of Exact Exchange. *J. Chem. Phys.* **1993**, *98* (7), 5648–5652. <https://doi.org/10.1063/1.464913>.
- (5) Lee, C.; Yang, W.; Parr, R. G. Development of the Colle-Salvetti Correlation-Energy Formula into a Functional of the Electron Density. *Phys. Rev. B* **1988**, *37* (2), 785–789. <https://doi.org/10.1103/PhysRevB.37.785>.
- (6) Chai, J.-D.; Head-Gordon, M. Long-Range Corrected Hybrid Density Functionals with Damped Atom-Atom Dispersion Corrections. *Phys. Chem. Chem. Phys. PCCP* **2008**, *10* (44), 6615–6620. <https://doi.org/10.1039/b810189b>.
- (7) Hirata, S.; Head-Gordon, M. Time-Dependent Density Functional Theory within the Tamm–Dancoff Approximation. *Chem. Phys. Lett.* **1999**, *314* (3–4), 291–299. [https://doi.org/10.1016/S0009-2614\(99\)01149-5](https://doi.org/10.1016/S0009-2614(99)01149-5).
- (8) Grimme, S.; Bannwarth, C.; Shushkov, P. A Robust and Accurate Tight-Binding Quantum Chemical Method for Structures, Vibrational Frequencies, and Noncovalent Interactions of Large Molecular Systems Parametrized for All Spd-Block Elements ($Z = 1\text{--}86$). *J. Chem. Theory Comput.* **2017**, *13* (5), 1989–2009. <https://doi.org/10.1021/acs.jctc.7b00118>.
- (9) Bannwarth, C.; Ehlert, S.; Grimme, S. GFN2-XTB—An Accurate and Broadly Parametrized Self-Consistent Tight-Binding Quantum Chemical Method with Multipole Electrostatics and Density-Dependent Dispersion Contributions. *J. Chem. Theory Comput.* **2019**, *15* (3), 1652–1671. <https://doi.org/10.1021/acs.jctc.8b01176>.
- (10) Sheldrick, G. M. A Short History of SHELX. *Acta Crystallogr. A* **2008**, *64* (1), 112–122. <https://doi.org/10.1107/S0108767307043930>.